

Review

# Preparation and Application of Green Sustainable Solvent Cyrene

Yadong Wang <sup>1,†</sup>, Mingfei Dai <sup>1,†</sup>, Gang Luo <sup>1,2</sup>, Jiajun Fan <sup>3</sup>, James H. Clark <sup>1,2,3</sup> and Shicheng Zhang <sup>1,2,\*</sup> 

<sup>1</sup> Shanghai Technical Service Platform for Pollution Control and Resource Utilization of Organic Wastes, Shanghai Key Laboratory of Atmospheric Particle Pollution and Prevention (LAP3), Department of Environmental Science and Engineering, Fudan University, Shanghai 200438, China; 22210740074@m.fudan.edu.cn (Y.W.); 21110740032@m.fudan.edu.cn (M.D.); gangl@fudan.edu.cn (G.L.); james.clark@york.ac.uk (J.H.C.)

<sup>2</sup> Shanghai Institute of Pollution Control and Ecological Security, Shanghai 200092, China

<sup>3</sup> CRCL, Green Chemistry Centre of Excellence, Department of Chemistry, University of York, York YO10 5DD, UK; alice.fan@york.ac.uk

\* Correspondence: zhangsc@fudan.edu.cn

† These authors contributed equally to this work.

**Abstract:** The bio-based solvent dihydrolevoglucosenone (Cyrene) is a green and sustainable alternative to petroleum-based dipolar aprotic solvents. Cyrene can be prepared from cellulose in a simple two-step process and can be produced in a variety of yields. Cyrene is compatible with a large number of reactions in the chemical industry and can be applied in organic chemistry, biocatalysis, materials chemistry, graphene and lignin processing, etc. It is also green, non-mutagenic and non-toxic, which makes it very promising for applications. In this paper, we have also screened all articles related to Cyrene on the Web of Science and visualised them through Cite Space.

**Keywords:** Cyrene; levoglucosanone; green chemistry



**Citation:** Wang, Y.; Dai, M.; Luo, G.; Fan, J.; Clark, J.H.; Zhang, S. Preparation and Application of Green Sustainable Solvent Cyrene. *Chemistry* **2023**, *5*, 2322–2346. <https://doi.org/10.3390/chemistry5040154>

Academic Editor: Mark Mascali

Received: 15 September 2023

Revised: 13 October 2023

Accepted: 18 October 2023

Published: 21 October 2023



**Copyright:** © 2023 by the authors. Licensee MDPI, Basel, Switzerland. This article is an open access article distributed under the terms and conditions of the Creative Commons Attribution (CC BY) license (<https://creativecommons.org/licenses/by/4.0/>).

## 1. Introduction

Solvents are ubiquitous throughout the chemical industry, but traditional dipolar aprotic solvents are still dominated by petroleum-based solvents, the feedstock of which is a non-renewable resource, and the use of petroleum-based solvents can cause harm to human and environmental health. Today, environmental health and safety issues are in the spotlight. Green chemistry, as a scientific and technological approach to sustainable development, is rapidly gaining wide attention and recognition. With the increasing awareness of environmental protection and sustainable development, the principles and methods of green chemistry have been widely used in various fields [1].

Bioethanol and glycerol can be used as alternative bio-based solvents for plasmonic compounds, 2-methyltetrahydrofuran as an alternative to medium-polar solvents and  $\gamma$ -Valerolactone as a biologically derived green solvent can be an alternative to polar aprotic solvents, but few bio-based solvents can be used as alternatives to dipolar aprotic solvents. Many of the traditional dipolar aprotic solvents, including sulpholane and amides such as *N*-methyl-2-pyrrolidone (NMP) and *N,N*-dimethylformamide (DMF), have been added to the REACH Restricted Substances List due to their toxicity, which severely limits their ability to be used as industrial solvents. Although Dimethyl sulfoxide (DMSO) is superior to DMF and NMP in applications, it still has potential safety hazards. Dihydrolevoglucosenone (Cyrene) is the best alternative to dipolar aprotic solvents [1–3]. This review focuses on Cyrene, with an emphasis on the preparation of Cyrene from cellulose as a feedstock and its application as a dipolar aprotic solvent to replace DMF and NMP in particular.

## 2. Literature Analysis Report

The topic Cyrene was searched in the Web of Science core database, after which 150 documents related to the green solvent dihydro levoglucosanone were manually screened and visualised using Citespace, analysing the cited documents, keywords, countries and journals [4–6].

Firstly, the temporal distribution of all the literature (Figure 1) was analysed through the Web of Science, and it was found that research on Cyrene started following Sherwood's original paper in 2014 [1] and increased year by year to reach its peak in 2022. Sherwood's article was the most cited, with 274 citations.

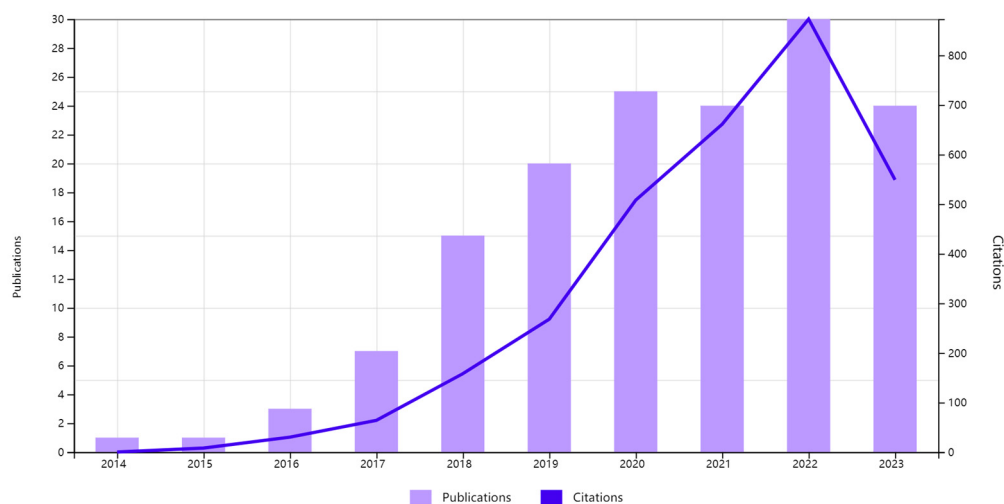


**Figure 1.** The temporal distribution of all the literature.

The co-citation of literature was first analysed by investigating the frequency of citations in order to identify the core literature that has a significant impact on the field of study. As shown in Figure 2, a node represents a document, and larger nodes indicate a higher citation frequency. Different colours indicate citations in different years. The most cited in the field of Cyrene is Zhang JF 2016, focusing on the application of Cyrene to the synthesis of metal-organic frameworks (MOFs) [7]. The second most cited article is Sherwood J 2014 which was also the first article on Cyrene [1]. These two articles have a key role to play in Cyrene's field.

If an article has a citation burst, this means that it has attracted scholarly attention at some point in time [5]. As shown in Table 1, the article with the strongest bursts was that of Zhang JF 2016, proving that the application of Cyrene in the preparation of MOFs was widely followed from 2017 to 2021 [7].

Keywords are important indicators for identifying hotspots in the research field [5]. Citespace employs algorithmic techniques for the purpose of clustering proximate keywords, each associated with a singular numerical value, wherein the maximal value within a cluster coincides with the designated label for a said cluster. In the network modularity,  $Q$  and Silhouette  $S$  denote the clustered module value and the clustered mean profile value, respectively;  $Q > 0.3$  implies a significant clustering structure,  $S > 0.5$  implies a reasonable clustering and  $S > 0.7$  implies a convincing clustering [8]. In Figure 3,  $Q = 0.7671$  and  $S = 0.9081$ , which indicates that the clustering structure is significant and the clustering is convincing. Figure 3 represents the main clusters of Cyrene, the largest of which is Sonogashira cross-coupling. Other major clusters are aza-Michael isomerisation, MOF synthesis, butyl acetate, serendipitous formation and surface interactions studies.

**Table 1.** Top 10 References with the strongest citation bursts.

References	Year	Strength	Begin	End	2014–2023
Sherwood J, 2014, CHEM COMMUN, V50, P9650, DOI 10.1039/c4cc04133j, DOI	2014	5.94	2016	2017	--- --
Alder CM, 2016, GREEN CHEM, V18, P3879, DOI 10.1039/c6gc00611f, DOI	2016	2.6	2016	2019	--- --
Zhang JF, 2016, ACS SUSTAIN CHEM ENG, V4, P7186, DOI 10.1021/acssuschemeng.6b02115, DOI	2016	6.64	2017	2021	--- --
Cao F, 2015, ENERG ENVIRON SCI, V8, P1808, DOI 10.1039/c5ee00353a, DOI	2015	5.85	2017	2018	--- --
Wilson KL, 2016, BEILSTEIN J ORG CHEM, V12, P2005, DOI 10.3762/bjoc.12.187, DOI	2016	4.3	2017	2020	--- --
Prat D, 2016, GREEN CHEM, V18, P288, DOI 10.1039/c5gc01008j, DOI	2016	3.08	2017	2021	--- --
De Bruyn M, 2016, ENERG ENVIRON SCI, V9, P2571, DOI 10.1039/c6ee01352j, DOI	2016	2.31	2017	2019	--- --
Byrne F, 2017, GREEN CHEM, V19, P3671, DOI 10.1039/c7gc01392b, DOI	2017	2.32	2018	2020	--- --
Sherwood J, 2016, GREEN CHEM, V18, P3990, DOI 10.1039/c6gc00932h, DOI	2016	2.71	2019	2020	--- --
Marino T, 2019, J MEMBRANE SCI, V580, P224, DOI 10.1016/j.memsci.2019.03.034, DOI	2019	2.34	2020	2021	--- --

CiteSpace, v. 6.2.R4 (64-bit) Basic  
 August 31, 2023 at 4:14:21 PM CST  
 WoS: C:\Users\hp\Desktop\WoS\data  
 Timespan: 2013-2023 (Slice Length=1)  
 Selection Criteria: g-index (k=18), LRF=3.0, L/N=10, LBY=5, e=1.0  
 Network: N=294, E=709 (Density=0.0165)  
 Largest 30 CCs: 294 (100%)  
 Nodes Labeled: 1.0%  
 Pruning: Pathfinder

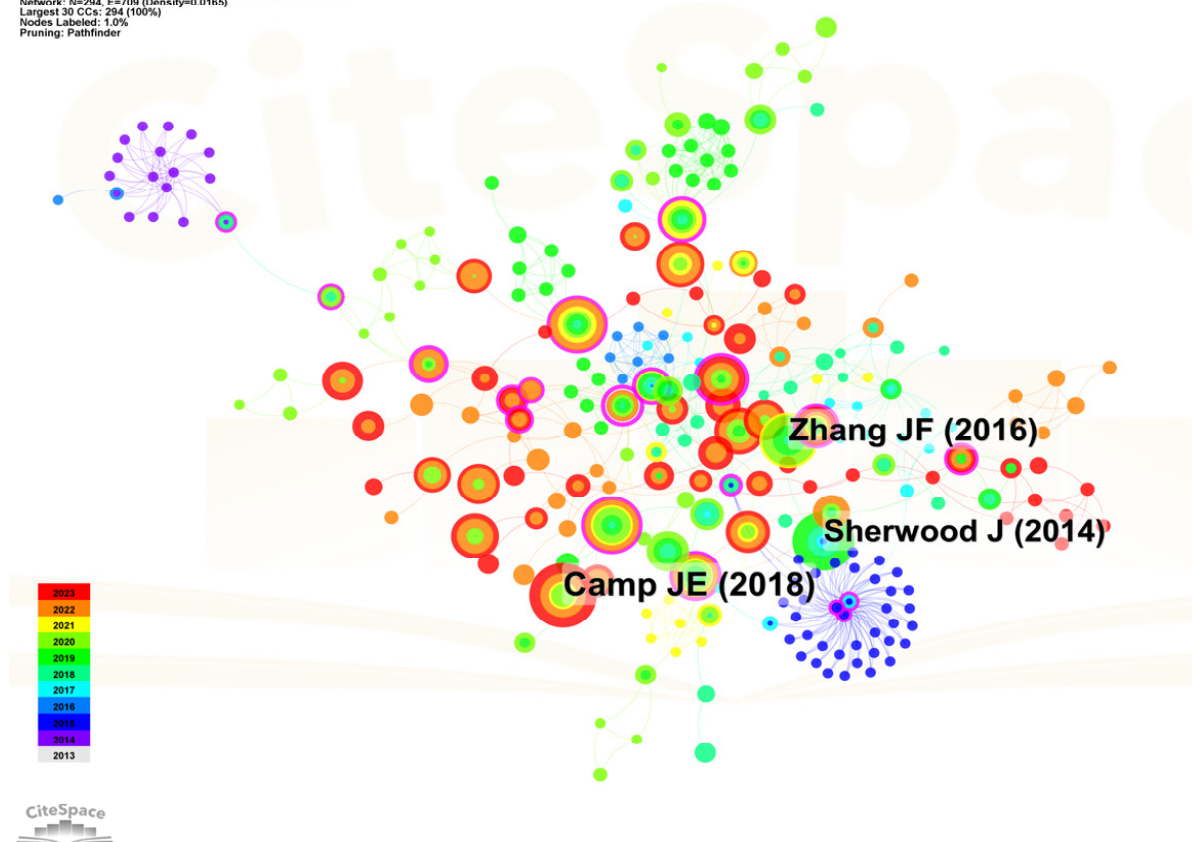
**Figure 2.** Co-citation network of articles [1,3,7].



Figure 3. Cluster analysis of the research keywords.

### 3. Preparation of Cyrene

The preparation of Cyrene is carried out in two steps (Figure 4): the first step is the catalytic pyrolysis of cellulose or cellulose-containing substances (e.g., pine, poplar, kraft pulp, newspaper, sawdust, etc.) to generate levoglucosanone (LGO), and in the second step, the catalytic hydrogenation of levoglucosanone to obtain Cyrene. Because the catalytic pyrolysis of cellulose is a very complicated reaction process, and the yield of the second step of catalytic hydrogenation of pure LGO is generally higher and can reach more than 90%, the main limitation of the preparation is the first step.

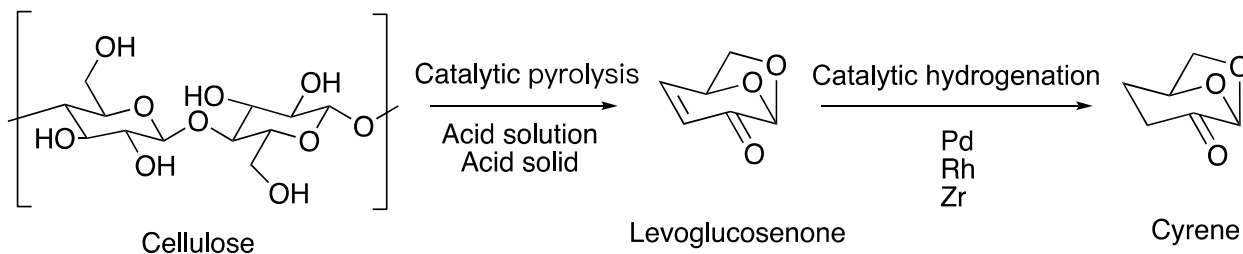
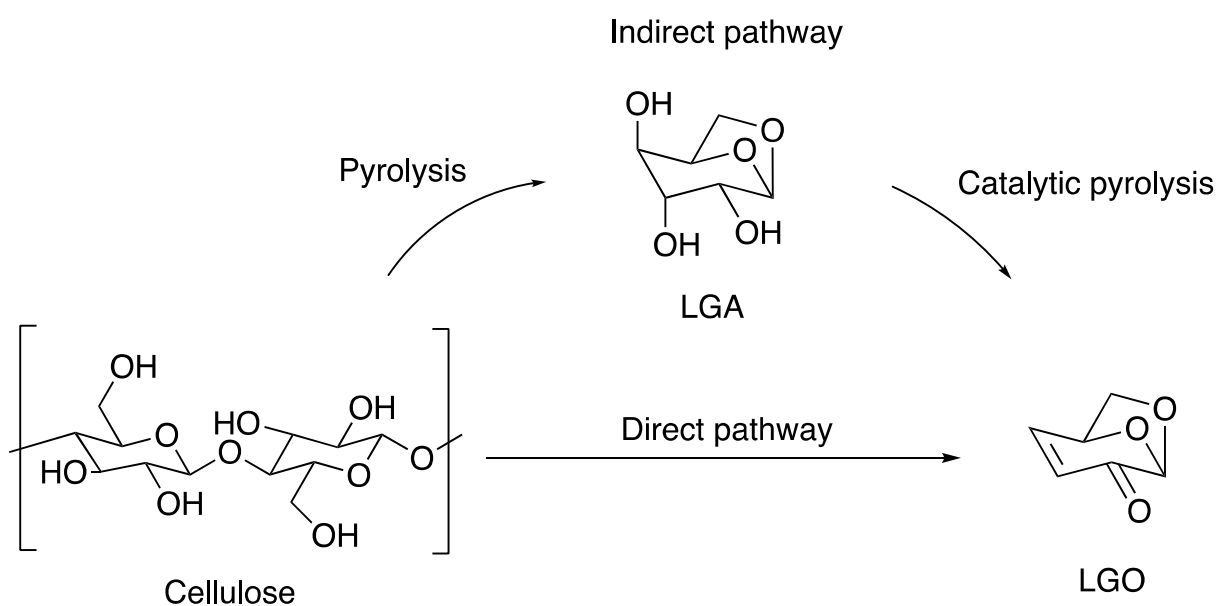


Figure 4. The process of preparing Cyrene with cellulose.

#### 3.1. Preparation of LGO

The preparation process for the catalytic pyrolysis of cellulose is divided into two main categories depending on the type of catalyst used: one is catalytic pyrolysis using an acid solution as the catalyst, and the other is pyrolysis using an acidic solid catalyst. The main product of cellulose pyrolysis without a catalyst is levoglucosan (LGA) with a yield of around 70%. The yield of LGO can be increased in the presence of an acid catalyst. Pyrolysis

using an acid solution as a catalyst is subdivided into two types: one in which the cellulose is pretreated by impregnation in an acid solution and then pyrolysed at atmospheric pressure, and the other in which the cellulose is pyrolysed in a solvent under high pressure. Kudo, through a comprehensive investigation of LGO preparation methods, classified LGO production strategies into three categories based on the catalytic technique employed (Figure 5): direct LGO production from cellulose pyrolysis after catalyst impregnation, catalytic pyrolysis in the gas phase using solid catalysts and catalytic pyrolysis in the liquid phase using liquid catalysts [9]. This is due to the fact that Lu et al. computed potential reaction pathways from  $\beta$ -D-glucopyranose and cellobiose to LGO using density functional theory (DFT) to derive the fact that LGA cannot be the essential intermediate of LGO [10]. Assary and Curtiss considered low yields or difficulties in the formation of LGO from LGA by quantitatively calculating the reaction energies and barriers [11]. They concluded that the reaction using catalyst impregnation followed by direct pyrolysis is a complex process for making LGO.



**Figure 5.** Cellulose conversion pathway to LGO.

### 3.1.1. Acid Impregnation Followed by Pyrolysis to Produce LGO Directly

As early as 1972, Halpern et al. obtained LGO by mixing cellulose with acidic additives and then pyrolysing it, isolating LGO in the product and determining its structure for the first time [12]. In 1998, Dobeles et al. impregnated cellulose with phosphoric acid at different concentrations and then pyrolysed it, finding that depolymerisation began to take place in the amorphous region of the cellulose at 250–300 °C, and depolymerisation also began to take place in the crystalline region at 325 °C [13]. The presence of phosphoric acid inhibits the formation of LGA and facilitates the conversion of cellulose to glucopyranose, the precursor of LGO, at 200–250 °C. The presence of sulfuric acid also acts as a catalyst for the formation of LGO, but phosphoric acid is more effective in catalysing the pyrolysis of cellulose. It was found that 5 wt% phosphoric acid was the optimal concentration, although the higher the concentration of phosphoric acid, the better the dehydration effect, but with more than 5% phosphoric acid, impregnation of cellulose condensed structures are formed, which can no longer be degraded to volatile monomers. By comparing the yields of different reaction feedstocks, it was found that the crystallinity of cellulose affects the accessibility of phosphoric acid, which indirectly affects the yield of LGO: a more ordered supramolecular structure of cellulose should be chosen as the feedstock if a high LGO yield is to be pursued [14–16]. Pyrolysis of cellulose using microwave radiation can also generate LGO, but the yield of 7.5% is lower than the traditional pyrolysis method [17].

It was previously found that the addition of iron to the pretreatment would lead to ions entering the cellulose by ion exchange or adsorption, thus promoting depolymerisation and dehydration reactions [15], leading to a further increase in the yield of LGO. Kudo et al. pretreated the cellulose in this way and reacted it using 1-butyl-2,3-dimethylimidazolium triflate ionic liquid, which is thermally stable and strongly catalytic obtaining a yield of 22 wt%, which is higher than that obtained by using pyrolysis after conventional acid impregnation [18]. Zandersons et al. used birch and pine as pyrolysis feedstocks for LGO production and found that elevated lignin content and total or partial elimination of hemicellulose contributed to the selective generation of LGO using phosphoric acid catalysis at 375 °C [19]. Pyrolysis of birch and pine wood using aqueous phosphoric acid at concentrations of 3.7 wt% and 3 wt%, respectively, as a catalyst yielded the highest LGO yields of 21.8% and 29%, which, when converted to cellulose as a feedstock, was found to be more than 55% using pine as a feedstock. Hydrothermal treatment of the feedstock followed by impregnation can increase the yield of LGO. Analytical pyrolysis of birch wood impregnated with 5 per cent phosphoric acid after hydrothermal treatment at 180 °C at 350 °C resulted in an LGO yield of 21.08% [20]. A lignin-rich biorefinery waste stream can also be used as a feedstock for the production of LGO. Selectivity to LGO is over 90%. Microwave-assisted pyrolysis using sulphuric acid as a catalyst at 180 °C only gave LGO yields up to 8 wt% [21]. The hemicellulose of barley straw was removed using microwave-assisted acid hydrolysis, followed by a combination of microwave-assisted pyrolysis and steam distillation of the wet samples to obtain the LGO [22]. Acid concentration was the most important factor affecting the distribution of the products, with LGO and LGA being the main products at low acid concentrations and furfural and levulinic acid being the main products at high acid concentrations. In situ vaporisation of water produces a microwave-transparent vapour environment that prevents further degradation of the distillation products.

### 3.1.2. Indirect Generation of LGO Using Solid Catalysts

In catalytic pyrolysis using solid catalysts, the solid catalysts do not act directly on the cellulose feedstock but further the catalytic pyrolysis of the initial pyrolysis products, such as LGA [9]. The advantage of using solid catalysts compared with acid impregnation methods lies in the fact that yields are much higher, and also the catalysts can be recovered for reuse. In the process of selective generation of LGO, two indicators of the solid catalyst have the greatest influence on the yield, the acidity and the porosity [23]. In 2011, Wang et al. used sulfated zirconia as a catalyst for the rapid pyrolysis of cellulose for the preparation of LGO, and the highest yield of 8.14% was attained at 335 °C with a ratio of  $\text{SO}_4^{2-}/\text{ZrO}_2$  of 3:3 [24]. The recycled catalyst still maintained the parent structure after recovery, but the activity decreased due to the leaching of  $\text{SO}_4^{2-}$ . Wei et al. similarly used  $\text{SO}_4^{2-}/\text{ZrO}_2$  and obtained a 7.25% yield of LGO: the pore size of the prepared catalysts was 10/40 nm. They also compared the effect of HZSM-5,  $\text{ZrO}_2$ ,  $\text{TiO}_2$  and  $\text{Al}_2\text{O}_3$  as catalysts for the rapid pyrolysis of cellulose to generate LGO. The calcined sulphuric acid catalysts compared with uncalcined catalysts impregnated with sulphuric acid activity increased significantly [25]. Lu et al. prepared magnetic super acid ( $\text{SO}_4^{2-}/\text{TiO}_2\text{-Fe}_3\text{O}_4$ ) for the catalytic fast pyrolysis of cellulose and poplar wood. The LGO yields of cellulose and poplar wood as feedstock were 15.43 wt% and 7.06 wt% at 300 °C with a 1:1 catalyst feedstock, respectively. Compared with the non-magnetic solid catalysts and phosphoric acid and sulphuric acid, the selective catalytic effect on LGO was better. And it was also found that the LGO yield from poplar wood was comparable to that from direct cellulose as feedstock, which indicated that other components in poplar wood (hemicellulose, lignin, etc.) had little effect on the inhibition of LGO pyrolysis formation [26]. Zhang et al. prepared solid phosphoric acid (SPA) catalysts with different carriers for the catalytic fast pyrolysis of poplar wood for the production of LGO. The highest LGO yield of 8.2 wt% (16.1 wt% when cellulose was used as a feedstock) was obtained at 300 °C with a biomass-to-catalyst ratio of 1 for the catalysts prepared based on SBA-15, which was higher than that when using phosphoric acid [27]. When

Al was loaded on the ordered mesoporous catalyst MCM-41 by Casoni et al., the LGO yield reached 53 wt% using cellulose as the feedstock at 400 °C [23]. Characterisation of different catalysts in the literature and comparison in combination with yields revealed that mesoporous catalysts enable free diffusion of cellulose primary pyrolysis molecules compared with catalysts with larger pore volumes and pore sizes, resulting in higher bio-oil yield. Catalysts with smaller pore sizes slowed down the diffusion of the generated anhydrous sugars into the gas phase, leading to re-polymerisation and accompanying char formation, so the 3.8 nm pore size Al-MCM-41 presented the best selectivity. Li et al. prepared the Ni-P-MCM-41 catalysts at 350 °C with Ni/P at 5 and catalyst/feedstock at 3 [28]. The yield reached 27.34 wt% for cellulose as feedstock and up to 14.30 wt% when pine wood was used as feedstock. Although MCM-41 catalysts have shown excellent yields in laboratory-scale processes, it is difficult to achieve mass production due to their instability. The advantage of phosphorus-molybdenum-tin mixed metal oxide (P-Mo/SnO<sub>2</sub>) as a catalyst for the selective generation of LGO lies in its reusability, with a maximum LGO yield of 17.98% using P-Mo/SnO<sub>2</sub> as a catalyst, and the yield of LGO remained above 10 wt% after five regenerations [29].

### 3.1.3. Indirect Generation of LGO by Pyrolysis in Liquid Phase

When cellulose is reacted in the liquid phase of aprotic solvent at high pressure, there are two main paths: one is in the presence of water in the system, where cellulose undergoes hydrolysis, with 5-HMF being the main product, and the second is in the absence of water, where cellulose undergoes pyrolysis to produce LGA, which is then converted to LGO [30]. Cellulose in sulfuric acid or phosphoric acid within a cyclic sulfone solution can also be used to obtain LGO. The further conversion of LGO to furfural requires water, so the removal of water generated under mild vacuum conditions can significantly improve LGO yield. Further conversion of LGO to furfural requires water, so removal of the resulting water under mild vacuum conditions can significantly increase the yield of LGO, which reached 38% using phosphoric acid as a catalyst for 2.5 min at 280 °C [31]. The use of GVL and THF as solvents also produced LGO selectively, but GVL promoted the conversion of LGO to HMF and LGO was degraded in GVL. LGO is stable in THF. The pyrolysis pathway of cellulose in THF is shown in Figure 6. A 51% yield of LGO was achieved after 30 min at 210 °C using THF sulphate solution as a catalyst [30]. Using high voltage alternating current (HVAC) as a plasma source in a polar aprotic solvent without external heating, in situ-generated hydrogen radicals contribute to cellulose depolymerisation and intermediate dehydration to form LGO. A 43% yield of levoglucosanone was obtained in GVL after 15 min of conversion using a voltage of 6 kV and a frequency of 6 kHz and in sulfone after 7 min using a voltage of 3.5 kV 40% yield. This method can be carried out at lower energy consumption compared with previous methods [32]. The preparation methods and associated yields of LGO are shown in Table 2.

**Table 2.** Methods for the preparation of LGO.

Entry	Materials	Catalyst	Conditions	Reactor	Yield	Ref
1	Cellulose	NaHSO <sub>4</sub>	Slow pyrolysis at 300 °C	Horizontal tube reactor	6.9%	[12]
2	Cellulose	5.4 wt% H <sub>3</sub> PO <sub>4</sub>	Slow pyrolysis at 350 °C	vertical flow reactor	22.3%	[13]
3	Cellulose	2 wt% H <sub>3</sub> PO <sub>4</sub>	Fast pyrolysis at 500 °C	CDS Pyroprobe 100	34%	[15]
4	Newsprint	1 wt% H <sub>3</sub> PO <sub>4</sub>	Fast pyrolysis at 500 °C	CDS Pyroprobe 100	21%	[15]
5	Kraft pulp	2 wt% H <sub>3</sub> PO <sub>4</sub>	Fast pyrolysis at 500 °C	CDS Pyroprobe 100	19%	[15]
6	Birchwood	2.5 wt% H <sub>3</sub> PO <sub>4</sub>	Fast pyrolysis at 500 °C	CDS Pyroprobe 100	17%	[15]
7	Cellulose	Ionic liquids	Slow pyrolysis at 300 °C	Horizontal reactor	38.2%	[18]
8	Cellulose	SO <sub>4</sub> <sup>2-</sup> /ZrO <sub>2</sub>	Fast pyrolysis at 335 °C	Vertical reactor	8.14%	[24]
9	Cellulose	HZSM-5	Fast pyrolysis at 335 °C	Vertical reactor	1.7%	[24]
10	Cellulose	TiO <sub>2</sub>	Fast pyrolysis at 335 °C	Vertical reactor	5%	[24]

Table 2. Cont.

Entry	Materials	Catalyst	Conditions	Reactor	Yield	Ref
11	Cellulose	SO <sub>4</sub> <sup>2-</sup> /TiO <sub>2</sub> -Fe <sub>3</sub> O <sub>4</sub>	Fast pyrolysis at 300 °C	CDS Pyroprobe 5200HP pyrolyser	15.43%	[26]
12	Poplar wood	SO <sub>4</sub> <sup>2-</sup> /TiO <sub>2</sub> -Fe <sub>3</sub> O <sub>4</sub>	Fast pyrolysis at 300 °C	CDS Pyroprobe 5200HP pyrolyser	7.06%	[26]
13	Cellulose	SPA	Fast pyrolysis at 280 °C	CDS Pyroprobe 5200HP pyrolyser	16.1%	[27]
14	Cellulose	Al-MCM-41	Fast pyrolysis at 400 °C	Vertical reactor	53%	[23]
15	Cellulose	Ni-P-MCM-41	Fast pyrolysis at 350 °C	Vertical reactor	21.4%	[28]
16	Pine wood	Ni-P-MCM-41	Fast pyrolysis at 350 °C	Vertical reactor	10.7%	[28]
17	Cellulose	P-Mo/SnO <sub>2</sub>	Fast pyrolysis at 300 °C	Micropyrolyser	18%	[29]
18	Cellulose	P-Mo/SnO <sub>2</sub>	Fast pyrolysis at 300 °C	Vertical reactor	12.7%	[29]
19	Cellulose	1 wt% H <sub>3</sub> PO <sub>4</sub>	In sulfolane at 200–280 °C	Round flask	38%	[31]
20	Cellulose	20 mM H <sub>2</sub> SO <sub>4</sub>	In THF at 210 °C	Hastelloy autoclave	51%	[30]
21	Cellulose	7 mM H <sub>2</sub> SO <sub>4</sub>	Plasma electrolysis in GVL at 160 °C	Round-bottom flask	43%	[32]
22	Brichwood	5 wt% H <sub>3</sub> PO <sub>4</sub>	Analytical pyrolysis at 350 °C	Micro Double-shot Pyrolyser	21.08%	[20]
23	Crude waste softwood hydrolysis lignin	H <sub>2</sub> SO <sub>4</sub>	Microwave-assisted pyrolysis at 180 °C	CEM 'Discover' MW generator	8%	[21]

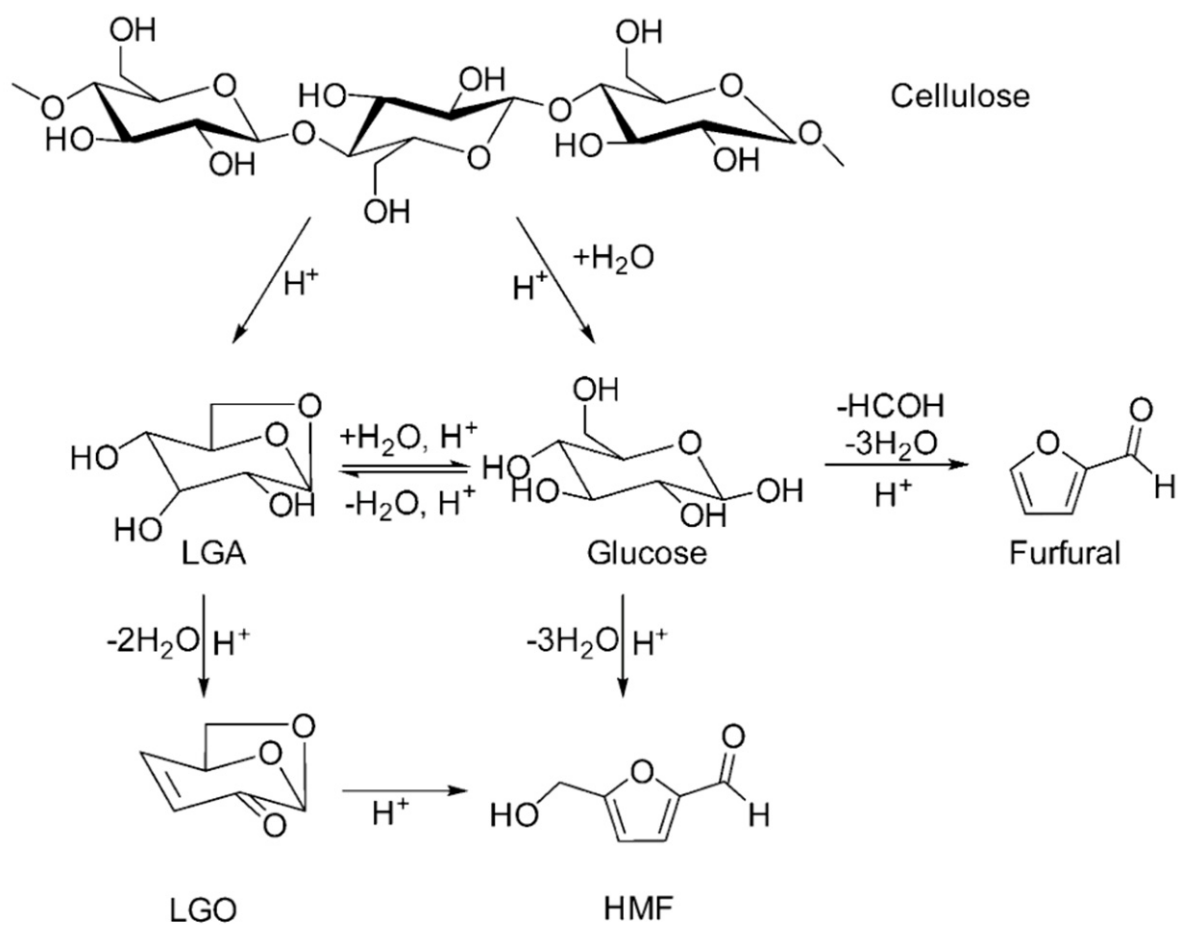


Figure 6. Cellulose pyrolysis pathway in THF [30].

### 3.2. Catalytic Hydrogenation of LGO to Produce Cyrene

Table 3 shows the method and yield for the preparation of Cyrene from LGO. In 2014, the Green Chemistry Centre of Excellence produced and named Cyrene as a solvent, and their catalytic hydrogenation of LGO was achieved under both low- and high-pressure conditions [1]. At low pressure, LGO is dissolved in ethyl acetate with 10 wt% Pd/C catalyst, and hydrogen is applied with a special Sigma Aldrich balloon for 96 h (8 days without solvent) to obtain Cyrene. At high pressure, the same solvent and catalyst are used to obtain Cyrene at room temperature for 2–48 h at pressures ranging from 3–80 bar. The reaction can be similarly completed in 2 h at 80 bar pressure without the addition of solvent [1]. Formic acid is a promising material for hydrogen storage and can be used as a substitute for hydrogen as a hydrogen source in the catalytic hydrogenation reaction of LGO [33]. In the paper, different catalysts (Ru/C, Rh/C, Pt/C, Pd/C, Ni) were also compared with different solvents (formic acid, cyclohexane, dimethylacetamide (DMA), 1,4-dioxane, 2-propanol and tetrahydrofuran), and it was finally found that the combination of THF and Pd/C showed the best performance in LGO hydrogenation, which could produce more than 99% yield at 66 °C. Pd/t-ZrO<sub>2</sub> (tetragonal ZrO<sub>2</sub>) has also been shown to have good catalytic performance, with a very low catalyst loading (~3 wt%) and the use of water as a solvent, achieving 95% yields of Cyrene. Reusability is also a key feature, with 90% Cyrene yield being achieved after a single use and thorough washing [34]. The conversion of LGO to Cyrene using wild-type Old Yellow Enzyme 2.6 (OYE 2.6 Tyr<sup>78</sup>Tt) from *Pichia* yeast and its mutant (OYE 2.6 Tyr<sup>78</sup>Trp) was 99%, and the biocatalysis through the enzymatic process of enzyme olefin reductase is low-toxicity, environmentally friendly and green [35]. In the conversion process of LGO to Cyrene, taken together, the yields can basically reach more than 99%. In summary, when using chemical catalysis, Pd/C as a catalyst and THF as a solvent = more than 99% = Cyrene can be achieved. For the hydrogen source, it is recommended to choose the more promising and greener formic acid, taking into account the toxicity of THF. We can also use non-toxic TMO as a solvent to replace THF [36].

**Table 3.** Methods for the preparation of Cyrene.

Entry	Catalyst	Solvent	Conditions	Reactor	Yield	Ref
1	10% Pd/C	/	1.1 atm H <sub>2</sub> , 8 days	/	>90%	[1]
2	10% Pd/C	EtOAc	1.1 atm H <sub>2</sub> , 96 h	/	>90%	[1]
3	10% Pd/C	EtOAc	3 to 80 bar, 2 to 48 h	High-pressure reactor	>90%	[1]
4	10% Pd/C	/	80 bar, less than 2 h	High-pressure reactor	>90%	[1]
5	5% Pd/C	THF	Stirring at 66 °C, 2 h	Autoclave	>99%	[33]
6	Pd/t-ZrO <sub>2</sub>	Water	10 bar H <sub>2</sub> , 80 °C	Batch glass micro-reactor	>99%	[34]
7	OYE 2.6 Tyr <sup>78</sup> Trp	EtOH	Room temperature	/	>99%	[37]

### 3.3. Furacell Process

Circa Group has achieved the large-scale mass production of Cyrene using the Furacell process. In this process (Figure 7) [37–39], the raw material is pine sawdust, the solvent is sulfone, and the catalyst is phosphoric acid. The pine sawdust was impregnated with a solution of sulfone containing phosphoric acid, and after mixing, it was put into a pyrolyser and heated rapidly to 330–350 °C under reduced pressure to separate the volatile products from the solid products and then separated the high purity LGO by several steps of distillation. Subsequently, compressed hydrogen is added to hydrogenate the LGO with a solid catalyst to obtain Cyrene. The purity of Cyrene generally depends on the purity of the separated LGO due to the 99% selectivity of the hydrogenation process. In this process, the separated biochar can be used as a fuel to provide energy for the pyrolysis process and can likewise be recycled as a by-product or sold as a fuel. Sulfone separated from LGO can be recycled many times, and the wastewater contains only water, acetic acid and furfural. Sulpholane can swell the cellulose so that the phosphoric acid can better penetrate into the

cellulose, improving the process, although the recent classification by the EU of sulfolane as a suspected reproductive toxin makes its continued use problematic.

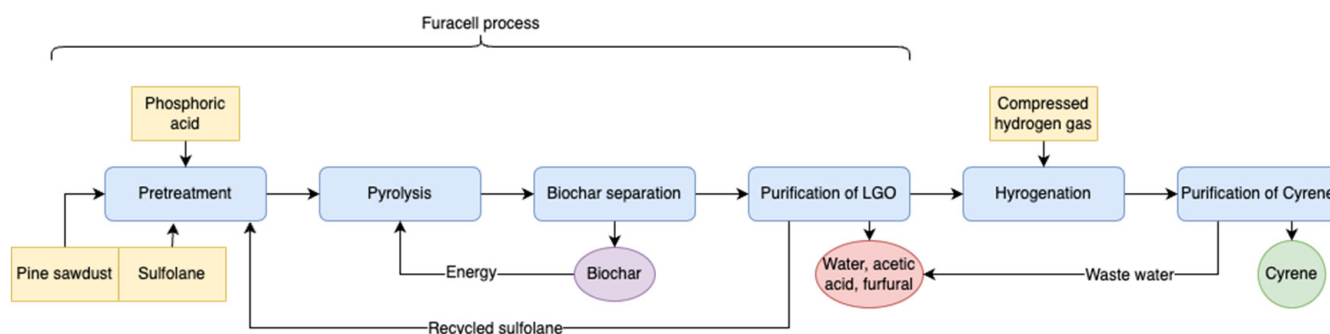


**Figure 7.** Potential pathways from LGA to LGO when pyrolysis in solvent.

#### 4. Applications of Cyrene

The application of Cyrene as a solvent was first reported less than 10 years ago [1]. This bio-based green solvent has been proposed as a bio-available replacement for *N*-methyl-2-pyrrolidone (NMP), dimethylformamide (DMF) and dimethylacetamide (DMAc), which are considered toxic organic solvents for the environment and human health [7]. Cyrene is becoming a more and more popular green and non-toxic reaction medium due to its compatibility as a solvent with plenty of reactions of great significance for the chemical industry. Indeed, Cyrene has enormous potential in traditional reactions in materials chemistry, organic chemistry, bio-catalysis and lignin manipulation [2,3].

##### 4.1. Cyrene for the Synthesis of Materials

###### 4.1.1. Cyrene in MOFs Synthesis

Katz et al. utilised Cyrene as a green solvent in comparison with DMF for the synthesis of metal-organic frameworks (MOFs) [7,40]. They synthesised five MOFs in Cyrene and compared their BET surface with MOF synthesised in DMF (Figure 8). They found that MOF synthesised in DMF had higher surface areas (SA), and the BET SA was about  $1400 \text{ m}^2 \text{ g}^{-1}$ , while the MOF's BET SA was  $600 \text{ m}^2 \text{ g}^{-1}$  in the mixture of Cyrene and EtOH. They figured out that the BET SA was  $1400 \text{ m}^2 \text{ g}^{-1}$  when dry ethanol was used as the additive with Cyrene. So, the authors examined various ratios of Cyrene/EtOH and the synthesis of other MOFs using Cyrene (Table 4). The authors pointed out that keeping the water content low and the short heating times are essential to synthesise Cyrene-based MOFs. Worrall et al. demonstrate the feasibility of replacing the traditional, toxic, fossil fuel-derived solvents in electrochemical MOF synthesis with safer, greener and cleaner alternatives. The use of bioderived solvents also provides a facile method for MOF phase selection during synthesis, with both more desirable higher porosity phases and, importantly, control over which phase is formed readily achieved [41]. Cyrene proved to successfully replace DMF in the synthesis of zeolitic imidazolate framework-90 (ZIF-90) [42].

**Table 4.** Obtained BET SA for MOFs [7].

Entry	MOFs	Expected ( $\text{m}^2 \text{g}^{-1}$ )	Observed in DMF ( $\text{m}^2 \text{g}^{-1}$ )	Observed in Cyrene ( $\text{m}^2 \text{g}^{-1}$ )
1	HKUST-1	1740	1400	1500
2	UiO-66	1700	1300	500
3	Co-MOF-74	1572	800	200
4	ZIF-8	1950	1700	600
5	$\text{Zn}_2(\text{BDC})_2(\text{DABCO})$	1750	1950	1300

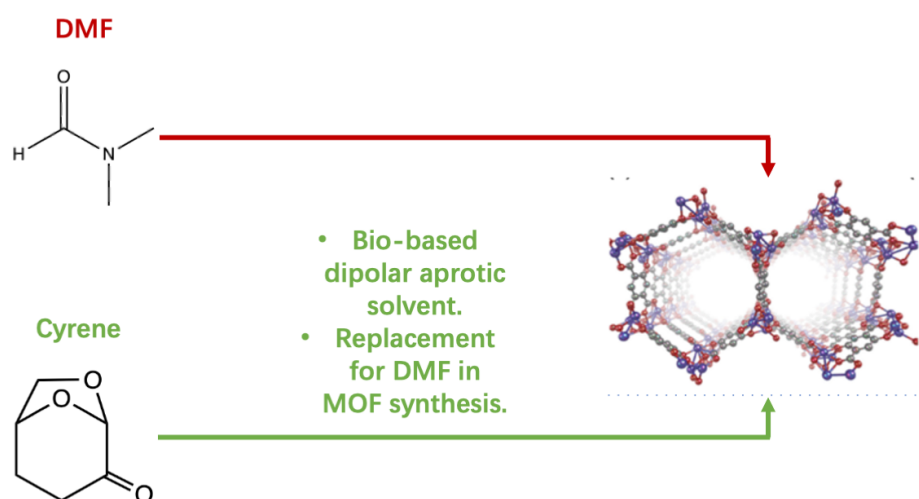


**Figure 8.** The replacement solvent strategy for MOF synthesis using Cyrene instead of DMF [7].

#### 4.1.2. Cyrene for the Fabrication of Membranes

The application of Cyrene for the fabrication of membranes is shown in Table 5. Figoli and coworkers developed a new sustainable approach for producing membranes by use of Cyrene [43]. Cyrene was proposed for the first time as a valuable bio-based solvent for the preparation of polyethersulfone (PES) and poly(vinylidene fluoride) (PVDF), which represent an excellent polymer for membrane preparation with well-established applications in micro-filtration (MF) and ultra-filtration (UF) membrane preparation. Clark et al. developed a more sustainable dialysis and water filtration membrane by using Cyrene in place of *N*-methyl pyrrolidinone (NMP), opening new perspectives for a more sustainable membrane fabrication [44]. They demonstrated that membranes fabricated with Cyrene showed higher overall porosity, bigger pore diameters and higher thermal stability compared with the PES membranes produced with NMP. In 2021, they explored a binary solvent system composed of biobased Cyrene and its derivative Cygnet 0.0 for application in membrane technology. Their mixture seemed to be more efficient as the solvent for the PES polymer. They pointed out that the temperature and the Cygnet–Cyrene analogy can determine the morphologies of the membranes, and different membranes could be formed with various properties and numerous applications [45]. Cyrene can also be used as a green solvent to test the separation performance and long-term stability of membranes [46,47]. Carner et al. first assessed the suitability of Cyrene for the fabrication of polymer inclusion membranes (PIMs) composed of the most commonly used polymers (poly(vinyl chloride) (PVC), cellulose triacetate and extractants). Because of this solvent's low volatility, the phase inversion technique was used for the casting of the corresponding PIMs. The PVC- and CTA-based PIMs cast with Cyrene were in homogeneous and opaque, but demonstrating the potential of Cyrene as a green solvent for the preparation of CTA-based PIMs [48]. Chai et al. investigated the feasibility and compatibility of fabricating membrane sheets with various green solvents (TEP, DMSO, Cyrene) and a conventional solvent (NMP), as a reference membrane. They conducted a comparison of membranes in the form of appearance, energy consumption and homogeneity of the dope solution [49]. In 2022, Gorgojo et al. first used Cyrene as a solvent for the fabrication of PES/GO membranes. The binodal lines, viscosity and final morphology of PES membranes prepared with NMP, DMAc, DMSO, DMF and Cyrene were studied [50]. During the same year, Paugam et al. developed a more sustainable and innovative method for the fabrication of polymeric membranes by a phase-inversion technique, Poly (hydroxybutyrate-cohydroxyvalerate) (PHBV) as the polymeric matrix and Cyrene as a green solvent [51].

**Table 5.** Cyrene for the fabrication of membranes.

Entry	Membranes	Conditions	Conclusions	Ref
1	PES, PVDF	13 wt% of PES/PVDF, 87 wt% Cyrene, exposure time to RH 0–5 min, NIPS and VIPS-NIPS.	Without pore former agent, Cyrene can be used for the preparation of PES and PVDF membranes.	[43]
2	PES, PVP	20 wt% PES, 0–7.6 wt% PVP 80 wt% Cyrene or NMP, 70 °C, 4 h, NIPS	With PVP and PEG, membranes produced with Cyrene are more sustainable, with less of both polymers' loss and tunable pore size and contact angles.	[44]
3	PVC/PIMs, PVDF-HFP/PIM	2 g CTA in 30 mL Cyrene, 50 °C, 3–4 days,	PVC dissolved at 60 °C with 30 mL solvent, PVDF-HFP not dissolved.	[48]
4	PES/GO	PES concentration 9%, GO concentration in the dope solution: 0.1, 0.3, 0.5	The highest porosity and pure water flux (PWF) occurs at a loading of 0.3 wt% GO for systems PES/GO/Cyrene.	[50]

#### 4.1.3. Cyrene for the Dispersion of Graphene and Carbon Nanotube

Clark et al. found that graphene dispersions in Cyrene were an order of magnitude higher than those achieved in NMP. Stable, high-concentration graphene dispersions in Cyrene mean shorter sonication times are possible, and less solvent is required. This could also improve conductivities and reduce process costs whilst maintaining the product's environmental credentials [52]. In 2018, Pan et al. reported the use of Cyrene to provide higher concentrations of graphene ink. In this work, highly conductive graphene ink ( $10 \text{ mg mL}^{-1}$ ) has been developed and was further concentrated to  $70 \text{ mg mL}^{-1}$  for screen printing [53]. Costa et al. developed environmentally friendly conductive polymer-based conductive inks reinforced with graphene-based polyvinylpyrrolidone (PVP) as the polymer binder and Cyrene as the solvent. Screen-printable inks are optimised in terms of viscosity and adhesion properties, leading to printed films with sheet resistance close to  $R_s = 1 \text{ k}\Omega \text{ sq}^{-1}$  [54]. Yang et al. reported a simple and environmentally friendly high-performance strain sensor based on a graphene/thermoplastic polyurethane (TPU) composite. The Cyrene was used to dissolve and disperse TPU and graphene to make conductive ink, and the graphene/TPU composite film was embedded in the polydimethylsiloxane (PDMS) matrix by stencil printing and transfer process [55]. Tkachev et al. proposed the preparation of graphene-based inks in Cyrene by a combination of two LPE methods. They produced highly concentrated dispersions (up to  $3.70 \text{ g L}^{-1}$ ) of few-layer graphene flakes (three to five layers) with a mean lateral size of  $\sim 200 \text{ nm}$  [56]. Among the possible options, Cyrene appears as the most promising green solvent for LPE techniques [57]. Poon and Zhitomirsky revealed a strong dispersion power of Cyrene and used Cyrene for the development of  $\text{Mn}_3\text{O}_4$ -multiwalled carbon nanotube (MWCNT) cathodes for supercapacitors [58]. Density functional theory was also used to investigate the microstructure formed by Cyrene on the surface of a Single-walled carbon nanotube (SWCNT). The orbital energy and influence of interaction energy on the van der Waals (vdW) interactions of Cyrene and ethylene glycol with SWCNT were examined and correlated with the dispersive forces within the fluid [59]. Exfoliation of graphene in Cyrene is shown in Table 6.

**Table 6.** Exfoliation of graphene in Cyrene.

Entry	Conditions	Conclusions	Ref
1	~4.5 mg of graphite, 3 mL Cyrene, ultrasonic mixed 15 min, exfoliation at 7000 rpm for 10 min 1 g TPU powder, 10 mL Cyrene,	92.5% of the flakes $\leq 10$ , 75% of the flakes $< 5\%$ , 7.5% are monolayer, $\leq 10$ layer flakes: $0.725 \pm 0.406 \mu\text{m}$ in width, $1.323 \pm 0.647 \mu\text{m}$ in length.	[52]
2	0.2 wt% fluorosurfactant 3000 rpm for 10 min, 1 g graphene was added, 3000 rpm for 10 min. For comparison, weight ratio of graphene to TPU at 1:2 and 2:1.	The graphene/TPU/PDMS wide tensile range ( $\sim 80\%$ ), excellent sensitivity ( $\text{GF} > 3905$ ), extremely low sensing limit ( $\sim 0.1 \%$ ) and good durability over 5000 cycles.	[55]
3	30 g of natural graphite powder, 600 mL Cyrene, 9000 rpm for 40 min.	Cyrene had the highest graphene flake concentration, smallest flake sizes and a generally narrower flake size distribution. Touch sensor prototype: optical transmittance of 78%, sheet resistance of $290 \Omega^{-1}$ and no significant change in sheet resistance when bent to a curvature radius of 28 mm.	[56]

#### 4.2. Cyrene for Extraction and Separation

In the past few years, researchers focused their research on the solubility of Cyrene. Clark et al. used Cyrene to extract hesperidin and rutin in a single-stage solid-liquid extraction. They found that the Cyrene is very effective when mildly heated to  $65 \text{ }^\circ\text{C}$  (up to 91%) or mixed with water. Adding water to Cyrene forms its geminal diol hydrate, and this enhances the solubility and extraction of hesperidin and rutin up to ten times compared with the original pure ketone form [37]. Meng et al. used a renewable cosolvent system, including Cyrene and water, to simultaneously achieve a good quality of carbohydrates and lignin. A near 100% cellulose conversion could be achieved for the enzymatic hydrolysis of Cyrene pretreated *Populus*. They also demonstrated that Cyrene pretreatment could be performed at a mild temperature ( $120 \text{ }^\circ\text{C}$ ) to reduce the lignin condensation and avoid significant cleavage of  $\beta\text{-O-4}$  linkages without compromising the lignin removal and solubility in the cosolvent system [60]. Coutinho et al. used COSMO-RS to rationalise the cosolvency effect of water on Cyrene. The study shows that water, when added in small quantities to Cyrene, acts as a cosolvent by preferentially interacting with the solute as a hydrogen bond acceptor, effectively doubling the hydrogen bond donating ability of the solute and thus maximising the interactions with Cyrene. In turn, this leads to a solubility increase of hydrophobic substances in wet Cyrene [61]. Mohan et al. employed multiscale molecular simulation approaches to understand the dissolution of lignin in Cyrene and Cyrene–cosolvent systems. They used the COSMO-RS model to assess the thermodynamic properties of lignin in Cyrene and Cyrene–cosolvent systems. From the COSMO-RS calculations, the correlation between the predicted activity coefficient and the experimental lignin solubility was excellent [62]. In 2022, Averous et al. evaluated the potential of Cyrene as an alternative polar aprotic solvent for lignins. They examined Cyrene's efficiency as a lignin solvent for lignins Kraft (KL), soda (SL) and organosolv (OSL). Cyrene is a promising and versatile green solvent for lignin fractionation, processing and chemistry [63]. Schuur et al. studied the extraction of low molecular weight polyhydroxyalkanoates from mixed microbial cultures using Cyrene. Cyrene-based extractions resulted in the highest yield of  $57 \pm 2\%$  with a purity of  $>99\%$  at  $120 \text{ }^\circ\text{C}$  in 2 h with a 5% (g/mL) biomass-to-solvent ratio. The mass balance closure over the extraction process indicated that about 10% of the polymer remained in the residual biomass after extraction Cyrene [64]. Wang et al. studied

the effects of pretreatment with  $\gamma$ -valerolactone/*p*-toluenesulfonic acid aqueous solution coupling system (GVL/TsOHaq) and Cyrene/*p*-toluenesulfonic acid aqueous solution coupling system (Cyrene/TsOH aq) on the chemical composition and enzymatic hydrolysis of maso bamboo [65,66]. Phaosiri et al. first used Cyrene and TMO for curcuminoid extraction. Cyrene provided a highly effective extraction yield among those tested [67]. Nejad et al. utilised Cyrene to dissolve the acetone insoluble lignin fraction to synthesize lignin-based polyurethane resin [68].

Thomas Brouwer and Boelo Schuur investigated the application of Cyrene in liquid–liquid extractions. The studies showed that there are certainly application windows for Cyrene in the case of oxygenate extraction. A process with Cyrene appears energy-saving [69]. They also compared the solvent-based affinity separation processes using Cyrene and sulfolane for aromatic/aliphatic separations [70]. Mumford et al. found that Cyrene is not a suitable solvent for liquid-liquid extraction for natural alkaloid extraction [71]. As a novel biosolvent, Cyrene shows more than promising features useful for designing greener and more sustainable methods for crystallisation, purification, extraction and formulation of bioactive compounds from natural sources. Extraction of hesperidin and rutin using Cyrene is shown in Table 7.

**Table 7.** Extraction of hesperidin and rutin using Cyrene.

Entry	Conditions	Solvent	Yield of Hesperidin		Solvent	Yield of Hesperidin		Ref
			RT	Hot		RT	Hot	
1	Orange peel: 250 mg black tea: 500 mg solvent: 5 mL stirred 2 min 14,450 rpm RT or 65 °C for 2 h	Cyrene	3.23	6.18	Cyrene + EtOH (43/57)	0.09	0.92	[37]
		Cyrene + EtOH (30/70)	11.61	/	Cyrene + MeOH (51/49)	0.34	1.54	
		Cyrene + H <sub>2</sub> O (70/30)	20.71	23.43	Cyrene + H <sub>2</sub> O (70/30)	1.53	1.68	
		Cyrene + Acetic add + H <sub>2</sub> O (49/22/29)	21.43	30.46	Cyrene + H <sub>2</sub> O (30/70)	1.52	1.17	

### 4.3. Cyrene in Chemical Synthesis

#### 4.3.1. Cyrene as a Reactant in Reactions

Wilson et al. described the scope and limitations of an alternative to DMF derived from renewable sources (Cyrene<sup>TM</sup>) in Sonogashira cross-coupling and Cacchi-type annulations (Figure 9) [72]. Alhifithi et al. investigated the reaction coordinate for the Beckmann reaction (normal Beckmann) and Beckmann fragmentation (abnormal Beckmann) manifest in the ground state. Uniquely, the Cyrene oximes show a lengthening of the C1–C2 bond upon increased leaving group ability and a greater magnitude of one-bond <sup>13</sup>C–<sup>13</sup>C coupling constants, supporting the divergence of mechanism for the normal and abnormal Beckmann reactions [73]. Hunt and coworkers reported Cyrene being successfully utilised as a bio-based platform molecule for the synthesis of pharmaceutically relevant intermediates through aldol condensation reactions and Claisen–Schmidt reactions (Figure 10) [74]. Allais et al. employed Cyrene<sup>®</sup> as a starting material for Bayer–Villiger oxidation to synthesise chemicals, such as drugs, pheromones, flavours and fragrances [75]. De Bruyn et al. have demonstrated that Cu and other metals supported on hydrotalcite can attain a high and stable catalytic activity for the hydrogenation of Cyrene, and this behaviour is independent of the exact pretreatment conditions [76]. Cyrene’s chiral chemical structure displays excellent selectivity in Diels–Alder reactions, sulfa-Michael reactions or diastereoselective Passerini reactions [77–80]. Mencer and coworkers prepared a library of exo-cyclic carbohydrate enones 2–13 via a base-catalysed, highly stereoselective aldol condensation of Cyrene with various aromatic aldehydes [81]. Cyrene has been transformed into its methacrylic derivative (m-Cyrene) for the first time, aiming at bio-based polymers [82,83]. Allais et al. first explored Cyrene as a green bio-alternative organic solvent for polymerisation (ROMP) reactions. The activity of the metathesis catalysts was finely tuned in Cyrene<sup>TM</sup> versus common and toxic solvents such as dichloromethane, resulting in highly thermostable functional polymers with a T<sub>d5%</sub> up to 401 °C and a T<sub>g</sub> of –16.8 °C (Figure 11) [84]. Kokotos et al. described a new, greener and more economical protocol for the Mizoroki–Heck reaction by using Cyrene as the green solvent and Pd/C as the palladium catalyst source.

A wide substrate scope for the coupling of aryl iodides with acrylamides, acrylates, acrylic acid, acrylonitrile and styrene was demonstrated. The recyclability of Cyrene and the leaching of palladium in the final product were examined in order to enhance the industrial applicability of this protocol [85].

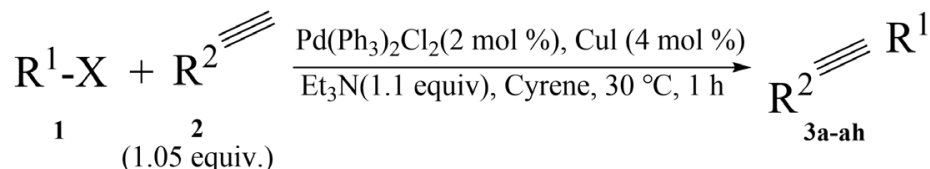


Figure 9. Cyrene-based Sonogashira cross-coupling [72].

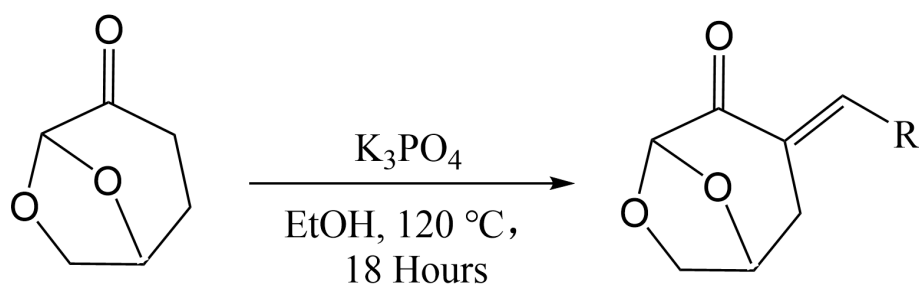


Figure 10. Claisen–Schmidt reaction between Cyrene and substrate [74].

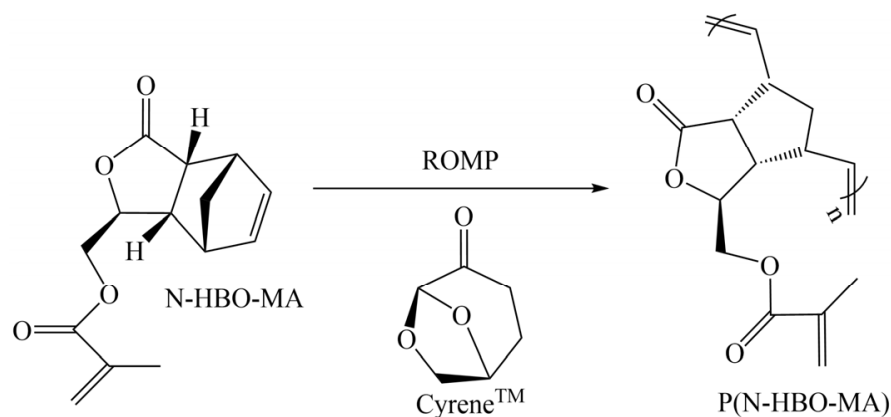


Figure 11. ROMP of N-HBO-MA in Cyrene™ [84].

#### 4.3.2. Cyrene as Replacement of Dipolar Aprotic Solvents in Reactions

Watson et al. were the first to use Cyrene to replace DMF as the solvent in a Pd-catalysed cross-coupling reaction [72]. Then, other researchers observed that Cyrene could be an excellent alternative medium for the Sonogashira cross-coupling reaction [86,87]. A greener alternative for the synthesis of ureas was proposed, and it was proven that Cyrene could possibly be used industrially as a solvent [88]. Watson and coworkers described the scope and utility of Cyrene in Suzuki–Miyaura cross-couplings and evaluated its suitability as a reaction medium for this benchmark transformation from discovery to gram scale in 2018 [89]. In 2020, James Sherwood evaluated the suitability of the Suzuki–Miyaura reaction to demonstrate the usefulness of new solvents, including Cyrene. He found that the cross-coupling is often unaffected by the choice of solvent, and therefore, the Suzuki–Miyaura reaction provides limited information regarding the usefulness of any particular solvent for organic synthesis [90]. Cyrene was found to be the most efficient solvent for the preparation of  $\beta$ - $\beta'$  dimers of sinapic acid derivatives. It also decreases the amount of pyridine used because it was used only as the oxidising agent [91,92]. Quero et al. studied the difluoromethylation of heteroarenes or terminal alkynes with Cyrene, which

replaced the NMP and DMF, leading to short reaction times and greater yields [93]. Meier et al. established a more sustainable synthesis protocol for the sulfurisation of isocyanides towards isothiocyanates using DBU as a greener catalyst in low loading down to 2 mol% and the green solvents Cyrene and GBL [94]. Hunt et al. studied the effectiveness of the green solvents *N*-butylpyrrolidinone (NBP),  $\gamma$ -valerolactone (GVL), propylene carbonate (PC) and dihydrolevoglucosenone (Cyrene) in Heck and Baylis–Hillman reactions. Cyrene exhibited high initial rates of reaction and high yields in the Baylis–Hillman reaction. This showed Cyrene to be a promising alternative polar aprotic solvent for this reaction [95].

#### 4.3.3. Cyrene Application in the Biomedical Field

Amide synthesis: amide bonds are one of the underpinning linkages in all living systems and are fundamental within drug discovery. Watson et al. evaluated the application of the bio-based solvent Cyrene™ in the HATU-mediated synthesis of amides and peptides (Figure 12). They found that Cyrene functioned as a competent replacement for DMF in the synthesis of a series of lead-like compounds and dipeptides [96]. In 2019, Camp et al. disclosed a waste-minimising and molar-efficient protocol for the synthesis of amides from acid chlorides and primary amines in Cyrene [97]. And the investigation into the hydration of Cyrene found that it readily hydrates to form a geminal diol in the presence of water with highly unusual properties and the ability to solubilize a wide range of organic compounds specifically and efficiently, notably, aspirin, ibuprofen, salicylic acid, ferulic acid, caffeine and mandelic acid (Figure 13). The possibility to tune the polarity of the solvent mixture through the addition of water and the subsequent generation of variable amounts of Cyrene's geminal diol creates a continuum of green solvents with controllable solubilisation properties [98,99]. Brook et al. reported a process to efficiently create a Ce6 dianhydride by the simple expedient usage of acetic anhydride as both a dehydrating agent and reagent. It was optimised for use with the greener solvent Cyrene, avoiding many difficulties and challenges [100].

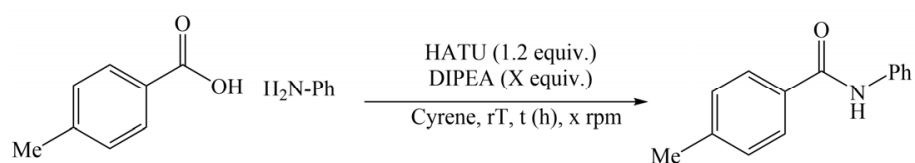


**Figure 12.** HATU mediated amide reaction [96].

In 2019, Cabri et al. attempted the solid-phase peptide synthesis with Cyrene and other green solvent binary mixtures. They found Cyrene was more efficient than the often-used solvents for peptide synthesis and proved that Cyrene might be a valuable green alternative for solid peptide synthesis (SPPS) [101,102].

Cyrene has been found to be slightly more toxic to bacteria of the ESKAPE pathogen set than DMSO. Scott et al. demonstrated the suitability of Cyrene as a replacement solvent for DMSO in antibacterial susceptibility testing. The MICs are shown in Table 8. They have also demonstrated, both qualitatively and quantitatively, that Cyrene and DMSO have comparable solubilising powers when used to prepare stock solutions of common antibacterial drugs [103]. The applications of Cyrene into a key precursor (*S*)- $\gamma$ -hydroxymethylbutyrolactone also be studied [104]. Biobased solvent Cyrene can substitute the reprotoxic NMP and potentially carcinogenic DCM solvents to synthesise the antidepressant and smoking cessation aid, bupropion hydrochloride [105].

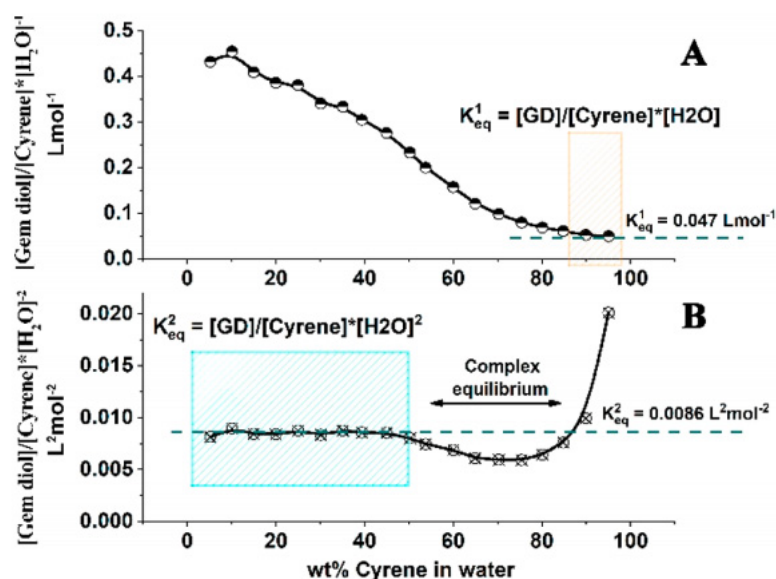


**Figure 13.** (A) Linearisation of the Cyrene–H<sub>2</sub>O solution compositional data based on the natural Cyrene–geminal diol equilibrium involving one water molecule; (B) linearisation of the Cyrene–H<sub>2</sub>O solution compositional data based on the involvement of two water molecules in the equilibrium [98].

**Table 8.** MIC<sub>80</sub> values of a panel of antibacterial drugs measured in either DMSO or Cyrene™ against the ESKAPE pathogens [103].

Compound	MIC <sub>80</sub> (μM)					
	<i>aureus</i>		<i>E. faecalis</i>		<i>E. coli</i>	
	DMSO	Cyrene	DMSO	Cyrene	DMSO	Cyrene
Tetracycline	0.78	0.78	NA	NA	3.13	3.13
Vancomycin hydrochloride	0.39	0.39	13	13	NA	NA
Ciprofloxacin hydrochloride	1.6	1.6	0.39	0.39	0.019	0.019
Colistin sulfate	NA	NA	NA	NA	0.78	0.78
Penicillin G sodium	34	34	NA	NA	NA	NA
Polymixin B sulfate	NA	NA	NA	NA	1.6	1.6
Tobramycin	NA	NA	NA	NA	0.78	0.78
Levofloxacin	0.78	0.78	0.19	0.39	0.019	0.019

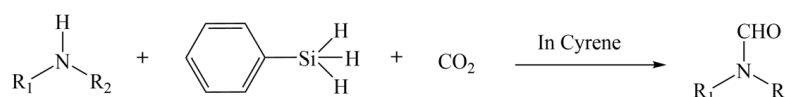
  

Compound	MIC <sub>80</sub> (μM)					
	<i>P. aeruginosa</i>		<i>A. baumannii</i>		<i>K. pneumoniae</i>	
	DMSO	Cyrene	DMSO	DMSO	Cyrene	DMSO
Tetracycline	25	25	25	25	25	25
Vancomycin hydrochloride	NA	NA	NA	NA	NA	NA
Ciprofloxacin hydrochloride	0.39	0.39	1.6	0.39	0.39	1.6
Colistin sulfate	3.1	3.1	1.6	3.1	3.1	1.6
Penicillin G sodium	NA	NA	NA	NA	NA	NA
Polymixin B sulfate	3.1	3.1	1.6	3.1	3.1	1.6
Tobramycin	1.6	1.6	3.1	1.6	1.6	3.1
Levofloxacin	1.6	1.6	0.39	1.6	1.6	0.39

#### 4.3.4. Cyrene Application in Biocatalysis

Cyrene has presented excellent results in biocatalysis, playing the role of the solvent and the catalyst simultaneously [106]. Witczak teams described the tereoselective synthesis

of exocyclic enones via a base-catalysed direct aldol condensation between Cyrene and heterocyclic aldehydes. The reaction is performed under mild conditions and is applicable to a variety of heterocyclic aldehydes [107]. In the next year, they prepared a library of exo-cyclic carbohydrate enones via a base-catalysed, highly stereoselective aldol condensation of Cyrene with various aromatic aldehydes [81]. Cellulose-derived was employed as a renewable catalytic solvent to convert CO<sub>2</sub>, and Yu teams found that Cyrene was highly efficient for reductive conversion of CO<sub>2</sub> with amines using PhSiH<sub>3</sub> as the reductant (Figure 14), and various corresponding formamides could be selectively synthesised [108]. Gonzalo employed Cyrene in biocatalysed reductions, employing purified alcohol dehydrogenase for the first time. A set of  $\alpha$ -ketoesters has been reduced to the corresponding chiral  $\alpha$ -hydroxyesters with high conversions and optical purities, making it possible to obtain good results at Cyrene contents of 30% *v/v* and working at substrate concentrations of 1.0 M in the presence of 2.5% *v/v* of this solvent [109]. Guajardo and Mariávvexplores used Cyrene in lipase-catalysed biotransformations, both in aqueous solutions, as a cosolvent, as well as non-conventional media for synthesis (Figure 15) [110]. Kuhl et al. describe the development of a protecting group-free, two-step synthesis of 1a from Cyrene<sup>TM</sup>, a biorenewable feedstock. The streamlined synthesis of 1a from Cyrene<sup>TM</sup> reduced the step count from nine to two synthetic steps, which resulted in a >27% yield improvement and a significant reduction in the environmental impact of the synthesis [111].



**Figure 14.** The *N*-formylation of amines with CO<sub>2</sub> in DLGO [108].

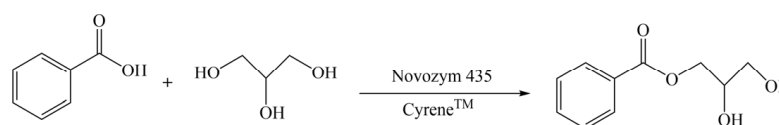


**Figure 15.** Lipase-catalysed esterification of benzoic acid and glycerol to obtain  $\alpha$ -MBG in Cyrene [110].

Under catalyst-free conditions, Lee and coworkers suggested the formation of bipyridine derivatives through a multicomponent reaction under microwave irradiation (Table 9). They use of Cyrene as the solvent enabled the researchers to attain an even higher yield than what was previously documented using DMF, as the temperature could be elevated without further problems [112].

**Table 9.** 2,3'-Bipyridine derivatives were formed with the initial reaction of aniline 1a with 3-formylchromone 2a and 2-pyridylacetonitrile (3a) under catalyst-free conditions and microwave irradiation [112].

Entry	Solvent	T [°C]	t [h]	Yield [a] [%]
1	-	90	2	40
2	H <sub>2</sub> O	90	1	-
3	EtOH	90	1	48
4	DMF	90	1	66
5	Cyrene <sup>TM</sup>	90	1	76
6	Cyrene <sup>TM</sup>	110	1	83
7	Cyrene <sup>TM</sup>	130	1	94
8	Cyrene <sup>TM</sup>	150	1	91
9 [b]	Cyrene <sup>TM</sup>	130	24	35
10	DMF	130	1	85
11	-	130	1	32

[a] Isolated yields. [b] Reaction under traditional heating.

#### 4.4. Cyrene for Non-Materials and Lithium-Ion Batteries Materials

In 2020, Szekely's group engineered nanocomposite hydrogels based on sustainable cellulose acetate for water treatment. They prepared the hydrogels using Cyrene via simple dropwise phase inversion. And they demonstrated the robustness and practicality of the nanocomposites in continuous environmental remediation by using the hydrogels to treat contaminated groundwater from the Adyar river in India [113]. To overcome the disadvantages like high viscosity and plasticising effects, Fischer et al. used Cyrene™ as a solvent, offering a simple, fast and non-toxic procedure to formulate poly(lactic-co-glycolic acid) (PLGA)-based nanoparticles (Table 10) [114,115]. Aqueous polymeric nanodispersions are suitable alternatives to reduce the use of organic solvents. German et al. reported that Cyrene demonstrates comparable performance to that of NMP as a cosolvent in the synthesis and the film-forming process of PUD [116]. Adam et al. calculated the interaction distances at equilibrium for different bacterial species and hydrophobic nanomaterials such as MoS<sub>2</sub> in two environmentally friendly solvents, water and Cyrene, and extended the Derjaguin, Landau, Verwey and Overbeek theory (DLVO theory) that describes the properties of nano-objects in solutions to the case of two-dimensional nanoflakes interacting with bacteria cell membranes, both for Gram-positive and Gram-negative bacteria [117]. Itawi et al. demonstrated the importance of Cyrene™ as a potential bio-based molecule to produce sustainable porous microparticles [118].

**Table 10.** Preparation of PLGA nanoparticles.

Entry	Conditions	Solvent	Yield	Ref
1	10 mg Resomer® RG 502, 1 mg atorvastatin Stirred 3 h, RT or 37 °C Homogenisation vs. ultrasonication (30 s, 1 and 2 min, 50% and 100% cycle)	Cyrene	60%	[114]
2	50 mg PLGA, Stirred 3 h, RT Homogenised at 24,000 rpm for 15 min	4.5 mL ethyl acetate + atorvastatin (5 mg) dissolved in poly(ethylene glycol) 400 g/mol as cosolvent	40%	

Belharouak et al. investigated a closed-loop recovery process to reclaim cathode materials, Al foils, and PVDF binder from cathode scraps using Cyrene. The Cyrene-based separation process embraces a sustainable electrode recovery and reuse platform and paves the way for battery recycling [119]. Whittingham et al. studied the possibility of using Cyrene to replace NMP for NMC 811 cathode fabrication. They found that although PVDF binder has very poor solubility in Cyrene at room temperature, increasing temperature can significantly change this. High-temperature (above 80 °C) electrode processing with Cyrene gives a promising performance, which is comparable to the conventional NMP fabricated electrode (Figure 16) [120].

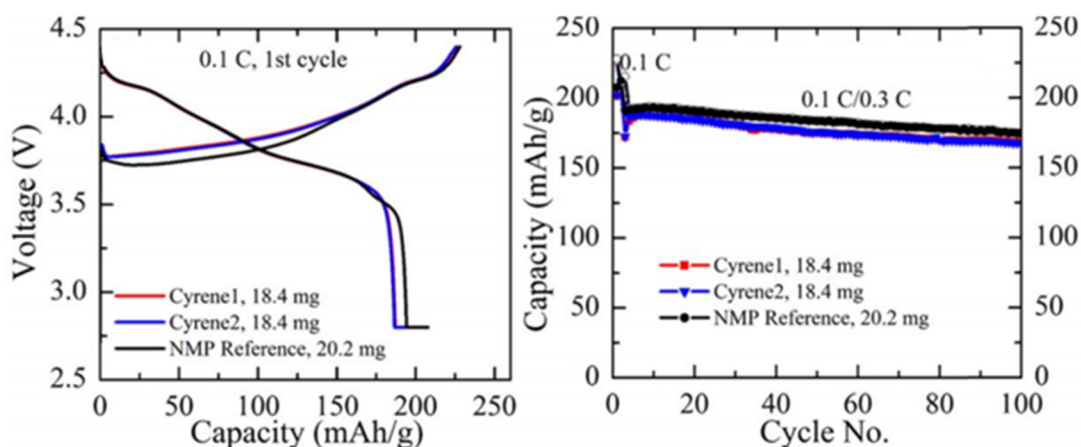


**Figure 16.** NMC 811 electrode fabricated with Cyrene as solvent of the electrode. First cycle and cyclability of the electrode compared with the conventional NMP fabricated electrode (black) [120].

## 5. Conclusions

The toxicity of the traditional dipolar aprotic solvents such as DMF and NMP has prompted the urgent need for safer solvents to replace them. Cyrene, which has similar properties, is an excellent alternative. Cyrene is sustainable when produced from biomass via LGO. In the production of LGO, the use of the acid impregnation and pyrolysis method is low-cost and has been industrialised, and the use of solid catalyst pyrolysis can give good yields, and the catalyst can be recycled. The catalytic hydrogenation of LGO gives a high conversion and can be stable and give high purity Cyrene. So, for the industrial production of Cyrene, prospects are very optimistic. Cyrene is becoming a more and more popular green, non-mutagenic and non-toxic reaction medium due to its compatibility as a solvent with many reactions of great significance for the chemical industry. Cyrene can be employed in everyday and traditional reactions in organic chemistry, biocatalysis, materials chemistry, graphene and lignin manipulation. We believe that further research can help solve any existing difficulties and give new data to develop significant new applications for this promising green solvent.

**Author Contributions:** Conceptualization, Y.W., M.D. and S.Z.; methodology, Y.W., M.D., J.H.C., J.F. and S.Z.; software, Y.W.; validation, Y.W., M.D., J.H.C. and S.Z.; formal analysis, Y.W., M.D., J.H.C., J.F. and S.Z.; investigation, Y.W. and M.D.; resources, Y.W. and M.D.; data curation, Y.W. and M.D.; writing—original draft preparation, Y.W. and M.D.; writing—review and editing, Y.W., M.D., J.H.C., J.F., G.L. and S.Z.; visualization, Y.W. and M.D.; supervision, S.Z.; project administration, S.Z.; funding acquisition, S.Z. All authors have read and agreed to the published version of the manuscript.

**Funding:** This research received no external funding.

**Data Availability Statement:** Data sharing not applicable. No new data were created or analyzed in this study. Data sharing is not applicable to this article.

**Conflicts of Interest:** The authors declare no conflict of interest.

## References

1. Sherwood, J.; De Bruyn, M.; Constantinou, A.; Moity, L.; McElroy, C.R.; Farmer, T.J.; Duncan, T.; Raverty, W.; Hunta, A.J.; Clark, J.H. Dihydrolevoglucosenone (Cyrene) as a bio-based alternative for dipolar aprotic solvents. *Chem. Commun.* **2014**, *50*, 9650–9652.
2. Stini, N.A.; Gkizis, P.L.; Kokotos, C.G. Cyrene: A bio-based novel and sustainable solvent for organic synthesis. *Green Chem.* **2022**, *24*, 6435–6449.
3. Camp, J.E. Bio-available Solvent Cyrene: Synthesis, Derivatization, and Applications. *ChemSusChem* **2018**, *11*, 3048–3055.
4. Chen, C. Searching for intellectual turning points: Progressive knowledge domain visualization. *Proc. Natl. Acad. Sci. USA* **2004**, *101*, 5303–5310. [PubMed]
5. Chen, C. CiteSpace II: Detecting and visualizing emerging trends and transient patterns in scientific literature. *J. Am. Soc. Inf. Sci. Technol.* **2006**, *57*, 359–377. [CrossRef]

6. Chen, C.; Leydesdorff, L. Patterns of connections and movements in dual-map overlays: A new method of publication portfolio analysis. *J. Assoc. Inf. Sci. Technol.* **2014**, *65*, 334–351.
7. Zhang, J.F.; White, G.B.; Ryan, M.D.; Hunt, A.J.; Katz, M.J. Dihydrolevoglucosenone (Cyrene) As a Green Alternative to N,N-Dimethylformamide (DMF) in MOF Synthesis. *ACS Sustain. Chem. Eng.* **2016**, *4*, 7186–7192. [[CrossRef](#)]
8. Chen, C. Science Mapping: A Systematic Review of the Literature. *J. Data Inf. Sci.* **2017**, *2*, 1–40.
9. Kudo, S.; Huang, X.; Asano, S.; Hayashi, J. Catalytic Strategies for Levoglucosenone Production by Pyrolysis of Cellulose and Lignocellulosic Biomass. *Energy Fuels* **2021**, *35*, 9809–9824.
10. Lu, Q.; Zhang, Y.; Dong, C.; Yang, Y.; Yu, H. The mechanism for the formation of levoglucosenone during pyrolysis of  $\beta$ -D-glucopyranose and cellobiose: A density functional theory study. *J. Anal. Appl. Pyrolysis* **2014**, *110*, 34–43.
11. Assary, R.S.; Curtiss, L.A. Thermochemistry and Reaction Barriers for the Formation of Levoglucosenone from Cellobiose. *ChemCatChem* **2012**, *4*, 200–205.
12. Halpern, Y.; Riffer, R.; Broido, A. Levoglucosenone (1,6-anhydro-3,4-dideoxy- $\Delta$ 3- $\beta$ -D-pyranosen-2-one). Major product of the acid-catalyzed pyrolysis of cellulose and related carbohydrates. *J. Org. Chem.* **1973**, *38*, 204–209.
13. Dobele, G.; Rossinskaja, G.; Telysheva, G.; Meier, D.; Faix, O. Cellulose dehydration and depolymerization reactions during pyrolysis in the presence of phosphoric acid. *J. Anal. Appl. Pyrolysis* **1999**, *49*, 307–317.
14. Dobele, G.; Meier, D.; Faix, O.; Radtke, S.; Rossinskaja, G.; Telysheva, G. Volatile products of catalytic flash pyrolysis of celluloses. *J. Anal. Appl. Pyrolysis* **2001**, *58–59*, 453–463. [[CrossRef](#)]
15. Dobele, G.; Dizhbite, T.; Rossinskaja, G.; Telysheva, G.; Meier, D.; Radtke, S.; Faix, O. Pre-treatment of biomass with phosphoric acid prior to fast pyrolysis: A promising method for obtaining 1,6-anhydrosaccharides in high yields. *J. Anal. Appl. Pyrolysis* **2003**, *68–69*, 197–211. [[CrossRef](#)]
16. Dobele, G.; Rossinskaja, G.; Dizhbite, T.; Telysheva, G.; Meier, D.; Faix, O. Application of catalysts for obtaining 1,6-anhydrosaccharides from cellulose and wood by fast pyrolysis. *J. Anal. Appl. Pyrolysis* **2005**, *74*, 401–405. [[CrossRef](#)]
17. Sarotti, A.M.; Spanevello, R.A.; Suárez, A.G. An efficient microwave-assisted green transformation of cellulose into levoglucosenone. Advantages of the use of an experimental design approach. *Green Chem.* **2007**, *9*, 1137–1140.
18. Kudo, S.; Zhou, Z.; Norinaga, K.; Hayashi, J. Efficient levoglucosenone production by catalytic pyrolysis of cellulose mixed with ionic liquid. *Green Chem.* **2011**, *13*, 3306–3311.
19. Zandersons, J.; Zhurinsh, A.; Dobele, G.; Jurkane, V.; Rizhikovs, J.; Spince, B.; Pazhe, A. Feasibility of broadening the feedstock choice for levoglucosenone production by acid pre-treatment of wood and catalytic pyrolysis of the obtained lignocellulose. *J. Anal. Appl. Pyrolysis* **2013**, *103*, 222–226.
20. Dobele, G.; Zhurinsh, A.; Volperts, A.; Jurkane, V.; Pomilovskis, R.; Meile, K. Study of levoglucosenone obtained in analytical pyrolysis and screw-type reactor, separation and distillation. *Wood Sci. Technol.* **2020**, *54*, 383–400.
21. Fan, J.; De Bruyn, M.; Budarin, V.L.; Gronnow, M.J.; Shuttleworth, P.S.; Breeden, S.; Macquarrie, D.J.; Clark, J.H. Direct Microwave-Assisted Hydrothermal Depolymerization of Cellulose. *J. Am. Chem. Soc.* **2013**, *135*, 11728–11731. [[PubMed](#)]
22. Bouxin, F.P.; Clark, J.H.; Fan, J.; Budarin, V. Combining steam distillation with microwave-assisted pyrolysis to maximise direct production of levoglucosenone from agricultural wastes. *Green Chem.* **2019**, *21*, 1282–1291.
23. Casoni, A.I.; Nievas, M.L.; Moyano, E.L.; Álvarez, M.; Diez, A.; Dennehy, M.; Volpe, M.A. Catalytic pyrolysis of cellulose using MCM-41 type catalysts. *Appl. Catal. A Gen.* **2016**, *514*, 235–240. [[CrossRef](#)]
24. Wang, Z.; Lu, Q.; Zhu, X.-F.; Zhang, Y. Catalytic Fast Pyrolysis of Cellulose to Prepare Levoglucosenone Using Sulfated Zirconia. *ChemSusChem* **2011**, *4*, 79–84.
25. Wei, X.; Wang, Z.; Wu, Y.; Yu, Z.; Jin, J.; Wu, K. Fast pyrolysis of cellulose with solid acid catalysts for levoglucosenone. *J. Anal. Appl. Pyrolysis* **2014**, *107*, 150–154. [[CrossRef](#)]
26. Lu, Q.; Ye, X.; Zhang, Z.; Dong, C.; Zhang, Y. Catalytic fast pyrolysis of cellulose and biomass to produce levoglucosenone using magnetic  $\text{SO}_4^{2-}/\text{TiO}_2\text{-Fe}_3\text{O}_4$ . *Bioresour. Technol.* **2014**, *171*, 10–15.
27. Zhang, Z.; Lu, Q.; Ye, X.; Wang, T.; Wang, X.; Dong, C. Selective Production of Levoglucosenone from Catalytic Fast Pyrolysis of Biomass Mechanically Mixed with Solid Phosphoric Acid Catalysts. *Bioenergy Res.* **2015**, *8*, 1263–1274.
28. Li, K.; Wang, B.; Bolatbieke, D.; Nan, D.-H.; Zhang, Z.-X.; Cui, M.-S.; Lu, Q. Catalytic fast pyrolysis of biomass with Ni-P-MCM-41 to selectively produce levoglucosenone. *J. Anal. Appl. Pyrolysis* **2020**, *148*, 104824.
29. Li, Y.; Hu, B.; Fu, H.; Wu, Y.; Zhang, Z.; Liu, J.; Zhang, B.; Lu, Q. Catalytic Fast Pyrolysis of Cellulose for the Selective Production of Levoglucosenone Using Phosphorus Molybdenum Tin Mixed Metal Oxides. *Energy Fuels* **2022**, *36*, 10251–10260. [[CrossRef](#)]
30. Cao, F.; Schwartz, T.J.; McClelland, D.J.; Krishna, S.H.; Dumesic, J.A.; Huber, G.W. Dehydration of cellulose to levoglucosenone using polar aprotic solvents. *Energy Environ. Sci.* **2015**, *8*, 1808–1815.
31. Kawamoto, H.; Saito, S.; Hatanaka, W.; Saka, S. Catalytic pyrolysis of cellulose in sulfolane with some acidic catalysts. *J. Wood Sci.* **2007**, *53*, 127–133. [[CrossRef](#)]
32. Lusi, A.; Radhakrishnan, H.; Hu, H.; Hu, H.; Bai, X. Plasma electrolysis of cellulose in polar aprotic solvents for production of levoglucosenone. *Green Chem.* **2020**, *22*, 7871–7883.
33. Huang, X.; Liu, T.; Wang, J.; Wei, F.; Ran, J.; Kudo, S. Selective hydrogenation of levoglucosenone over Pd/C using formic acid as a hydrogen source. *J. Energy Inst.* **2020**, *93*, 2505–2510. [[CrossRef](#)]

34. Mazarío, J.; Romero, M.P.; Concepción, P.; Chávez-Sifontes, M.; Spanevello, R.A.; Comba, M.B.; Suárez, A.G.; Domine, M.E. Tuning zirconia-supported metal catalysts for selective one-step hydrogenation of levoglucosanone. *Green Chem.* **2019**, *21*, 4769–4785. [[CrossRef](#)]
35. Mouterde, L.M.M.; Allais, F.; Stewart, J.D. Enzymatic reduction of levoglucosenone by an alkene reductase (OYE 2.6): A sustainable metal- and dihydrogen-free access to the bio-based solvent Cyrene (R). *Green Chem.* **2018**, *20*, 5528–5532. [[CrossRef](#)]
36. Byrne, F.; Forier, B.; Bossaert, G.; Hoebbers, C.; Farmer, T.J.; Clark, J.H.; Hunt, A.J. 2,2,5,5-Tetramethyltetrahydrofuran (TMTHF): A non-polar, non-peroxide forming ether replacement for hazardous hydrocarbon solvents. *Green Chem.* **2017**, *19*, 3671–3678. [[CrossRef](#)]
37. Milescu, R.A.; Segatto, M.L.; Stahl, A.; McElroy, C.R.; Farmer, T.J.; Clark, J.H.; Zuin, V.G. Sustainable Single-Stage Solid–Liquid Extraction of Hesperidin and Rutin from Agro-Products Using Cyrene. *ACS Sustain. Chem. Eng.* **2020**, *8*, 18245–18257. [[CrossRef](#)]
38. Richardson, D.E.; Raverty, W.D. Predicted environmental effects from liquid emissions in the manufacture of levoglucosenone and Cyrene (TM). *Appita* **2016**, *69*, 344–351.
39. Court, G.R.; Lawrence, C.H.; Raverty, W.D.; Duncan, A.J. Method for Converting Lignocellulosic Materials into Useful Chemicals. U.S. Patent 2012/0111714 A1, 6 January 2012.
40. El-Sayed, E.S.; Yuan, D. Waste to MOFs: Sustainable linker, metal, and solvent sources for value-added MOF synthesis and applications. *Green Chem.* **2020**, *22*, 4082. [[CrossRef](#)]
41. Bhindi, M.; Massengo, L.; Hammerton, J.; Derry, M.J.; Worrall, S.D. Structure Control Using Bioderived Solvents in Electrochemical Metal–Organic Framework Synthesis. *Appl. Sci.* **2023**, *13*, 720. [[CrossRef](#)]
42. Škrjanc, A.; Byrne, C.; Logar, N.Z. Green Solvents as an Alternative to DMF in ZIF-90 Synthesis. *Molecules* **2021**, *26*, 1573.
43. Marinoa, T.; Galianoa, F.; Molinob, A.; Figol, A. New frontiers in sustainable membrane preparation: Cyrene<sup>TM</sup> as green bioderived solvent. *J. Membr. Sci.* **2019**, *580*, 224–234. [[CrossRef](#)]
44. Milescu, R.A.; McElroy, C.R.; Farmer, T.J.; Williams, P.M.; Walters, M.J.; Clark, J.H. Fabrication of PES/PVP water filtration membranes using Cyrene<sup>®</sup>, a safer bio-based polar aprotic solvent. *Adv. Polym. Technol.* **2019**, *15*, 9692859. [[CrossRef](#)]
45. Milescu, R.A.; Zhenova, A.; Vastano, M.; Gammons, R.; Lin, S.; Lau, C.H.; Clark, J.H.; McElroy, C.R.; Pellis, A. Polymer Chemistry Applications of Cyrene and its Derivative Cygnet 0.0 as Safer Replacements for Polar Aprotic Solvents. *ChemSusChem* **2021**, *14*, 3367–3381. [[CrossRef](#)]
46. Le Phuong, H.A.; Izzati Ayob, N.A.; Blanford, C.F.; Mohammad Rawi, N.F.; Szekely, G. Nonwoven Membrane supports from Renewable Resources: Bamboo Fiber Reinforced Poly(Lactic Acid) Composites. *ACS Sustain. Chem. Eng.* **2019**, *7*, 11885–11893. [[CrossRef](#)]
47. Fei, F.; Le Phuong, H.A.; Blanford, C.F.; Szekely, G. Tailoring the Performance of Organic Solvent Nanofiltration Membranes with Biophenol Coatings. *ACS Appl. Polym. Mater.* **2019**, *1*, 452–460. [[CrossRef](#)]
48. Carner, C.A.; Croft, C.F.; Kolev, S.D.; Almeida, M.I.G.S. Green solvents for the fabrication of polymer inclusion membranes (PIMs). *Sep. Purif. Technol.* **2020**, *239*, 116486. [[CrossRef](#)]
49. Foong, Y.X.; Yew, L.H.; Chai, P.V. Green approaches to polysulfone based membrane preparation via dimethyl sulfoxide and eco-friendly natural additive gum Arabic. *Mater. Today Proc.* **2021**, *46*, 2092–2097. [[CrossRef](#)]
50. Mohsenpour, S.; Leaper, S.; Shokri, J.; Alberto, M.; Gorgojo, P. Effect of graphene oxide in the formation of polymeric asymmetric membranes via phase inversion. *J. Membr. Sci.* **2022**, *641*, 119924. [[CrossRef](#)]
51. Tomietto, P.; Russo, F.; Galiano, F.; Loulergue, P.; Salerno, S.; Paugam, L.; Audic, J.L.; De Bartolo, L.; Figoli, A. Sustainable fabrication and pervaporation application of bio-based membranes: Combining a polyhydroxyalkanoate (PHA) as biopolymer and Cyrene<sup>TM</sup> as green solvent. *J. Membr. Sci.* **2022**, *643*, 120061. [[CrossRef](#)]
52. Salavagione, H.J.; Sherwood, J.; Budarin, V.L.; Ellis, G.J.; Clark, J.H.; Shuttleworth, P.S. Identification of high performance solvents for the sustainable processing of graphene. *Green Chem.* **2017**, *19*, 2550. [[CrossRef](#)]
53. Pan, K.W.; Fan, Y.Y.; Hu, Z.R.; Leng, T.; Li, J.; Xin, Z.Y.; Zhang, J.W.; Hao, L.; Gallop, J.; Novoselov, K.S. Sustainable production of highly conductive multilayer graphene ink for wireless connectivity and IoT applications. *Nat. Commun.* **2018**, *9*, 5197–5206. [[CrossRef](#)] [[PubMed](#)]
54. Franco, M.; Motealleh, A.; Costa, C.M.; Hilliou, L.; Perinka, N.; Ribeiro, C.; Viana, J.C.; Costa, P.; Mendez, S.L. Environmentally Friendly Conductive Screen-Printable Inks Based on N-Doped Graphene and Polyvinylpyrrolidone. *Adv. Eng. Mater.* **2022**, *24*, 2101258. [[CrossRef](#)]
55. Yang, J.L.; Ling, K.; Liu, L.H.; Zeng, X.H.; Xu, X.W.; Li, Z.L.; He, P. Printable and Wearable Graphene-Based Strain Sensor With High Sensitivity for Human Motion Monitoring. *IEEE Sens. J.* **2022**, *22*, 14. [[CrossRef](#)]
56. Tkachev, S.; Monteiro, M.; Santos, J.; Placidi, E.; Hassine, M.B.; Marques, P.; Ferreira, P.; Alpuim, P.; Capasso, A. Environmentally Friendly Graphene Inks for Touch Screen Sensors. *Adv. Funct. Mater.* **2021**, *31*, 3287. [[CrossRef](#)]
57. Fernandes, J.; Nemala, S.S.; Bellis, G.D.; Capasso, A. Green Solvents for the Liquid Phase Exfoliation Production of Graphene: The Promising Case of Cyrene. *Front. Chem.* **2022**, *10*, 878799. [[CrossRef](#)]
58. Poon, R.; Zhitomirsky, I. Application of Cyrene as a solvent and dispersing agent for fabrication of Mn<sub>3</sub>O<sub>4</sub>-carbon nanotube supercapacitor electrodes. *Colloid Interface Sci.* **2020**, *34*, 100226. [[CrossRef](#)]
59. Das, N.K.; Mishra, D.K.; Banerjee, T.; Naik, P.K.; Dehury, P.; Bose, S.; Banerjee, T. Dihydrolevoglycosenone as a novel bio-based nanofluid for thermal energy storage: Physiochemical and quantum chemical insights. *J. Energy Storage* **2023**, *59*, 106365. [[CrossRef](#)]

60. Meng, X.Z.; Pu, Y.Q.; Ragauskas, A.J.; Lic, M.; Ragauskas, A.J. A biomass pretreatment using cellulose-derived solvent Cyrene. *Green Chem.* **2020**, *22*, 2862. [[CrossRef](#)]
61. Abranches, D.O.; Benfica, J.; Coutinho, J.A.P.; Abranches, D.O.; Shimizu, J.B.S.; Coutinho, J.A.P. Solubility Enhancement of Hydrophobic Substances in Water/Cyrene Mixtures: A Computational Study. *Ind. Eng. Chem. Res.* **2020**, *59*, 18247–18253. [[CrossRef](#)]
62. Mohan, M.; Sale, K.L.; Kalb, R.S.; Simmons, B.A.; Gladden, J.M.; Singh, S. Multiscale Molecular Simulation Strategies for Understanding the Delignification Mechanism of Biomass in Cyrene. *ACS Sustain. Chem. Eng.* **2022**, *10*, 11016–11029. [[CrossRef](#)]
63. Duval, A.; Averous, L. Dihydrolevoglucosenone (Cyrene™) as a versatile biobased solvent for lignin fractionation, processing, and chemistry. *Green Chem.* **2022**, *24*, 338–349. [[CrossRef](#)]
64. Elhami, V.; Beek, N.; Wang, L.S.; Picken, S.J.; Tamis, J.; Sousa, J.A.B.; Hempenius, M.A.; Schuur, B. Extraction of low molecular weight polyhydroxyalkanoates from mixed microbial cultures using bio-based solvents. *Sep. Purif. Technol.* **2022**, *299*, 121773. [[CrossRef](#)]
65. Yin, X.Y.; Cai, T.T.; Liu, C.; Jiang, J.C.; Wang, K. Directional Decomposition of Bamboo Powder in Bio-based Polar Aprotic Solvent / Aqueous p-Toluenesulfonic Acid Coupling Systems. *Chem. Ind. For. Prod.* **2022**, *1*, 0253–2417.
66. Yin, X.Y.; Cai, T.T.; Wang, K. A novel solvothermal biorefinery for production of lignocellulosic xylooligosaccharides, fermentable sugars and lignin nano-particles in biphasic system. *Carbohydr. Polym.* **2022**, *295*, 119901. [[CrossRef](#)]
67. Kisanthiaa, R.; Huntb, A.J.; Sherwoodc, J.; Somsakeesitd, L.; Phaosiri, C. Impact of conventional and sustainable solvents on the yield, selectivity and recovery of curcuminoids from turmeric. *ACS Sustain. Chem. Eng.* **2021**, *10*, 104–114. [[CrossRef](#)]
68. Arefmanesh, M.; Nikafshar, S.; Master, E.R.; Nejad, M. From acetone fractionation to lignin-based phenolic and polyurethane resins. *Ind. Crops Prod.* **2022**, *178*, 114604. [[CrossRef](#)]
69. Brouwer, T.; Schuur, B. Dihydrolevoglucosenone (Cyrene), a Biobased Solvent for Liquid-Liquid Extraction Applications. *ACS Sustain. Chem. Eng.* **2020**, *8*, 14807–14817. [[CrossRef](#)]
70. Brouwer, T. Schuur, Comparison of solvent-based affinity separation processes using Cyrene and Sulfolane for aromatic/aliphatic separations. *J. Chem. Tech. Biotech.* **2021**, *96*, 2630–2646. [[CrossRef](#)]
71. Wu, Y.; Li, W.; Vovers, J.; Lu, H.T.; Stevens, G.W.; Mumford, K.A. Investigation of green solvents for the extraction of phenol and natural alkaloids: Solvent and extractant selection. *Chem. Eng. J.* **2022**, *442*, 136054. [[CrossRef](#)]
72. Wilson, K.L.; Kennedy, A.R.; Murray, J.; Greatrex, B.; Jamieson, C.; Watson, A.J.B. Scope and limitations of a DMF bio-alternative within Sonogashira cross-coupling and Cacchi-type annulation. *Org. Chem.* **2016**, *12*, 2005–2011.
73. Alhifthi, A.; Harris, B.L.; Goerigk, L.; White, J.M.; Williams, S.J. Structure–reactivity correlations of the abnormal Beckmann reaction of dihydrolevoglucosenone oxime. *Org. Biomol. Chem.* **2017**, *15*, 10105–10115. [[CrossRef](#)]
74. Hughes, L.; McElroy, C.R.; Whitwood, A.C.; Hun, A.J. Development of pharmaceutically relevant bio-based intermediates through aldol condensation and Claisen-Schmidt reactions of dihydrolevoglucosenone (Cyrene®). *Green Chem.* **2018**, *20*, 4423–4427. [[CrossRef](#)]
75. Bonneau, G.; Peru, A.M.; Flourat, A.L.; Allais, F. Organic solvent- and catalyst-free Baeyer–Villiger oxidation of levoglucosenone and dihydrolevoglucosenone (Cyrene®): A sustainable route to (S)- $\gamma$ -hydroxymethyl- $\alpha,\beta$ -butenolide and (S)- $\gamma$ -hydroxymethyl- $\gamma$ -butyrolactone. *Green Chem.* **2018**, *20*, 2455–2458. [[CrossRef](#)]
76. Bruyn, M.D.; Sener, C.; Petrolini, D.D.; McClelland, D.J.; He, J.Y.; Ball, M.R.; Liu, Y.F.; Martins, L.; Dumesic, J.A.; Huber, G.W.; et al. Catalytic hydrogenation of dihydrolevoglucosenone to levoglucosan with a hydrotalcite/mixed oxide copper catalyst. *Green Chem.* **2019**, *21*, 5000–5007. [[CrossRef](#)]
77. Klepp, J.; Sumbly, C.J.; Greatrex, B.W. Synthesis of a Chiral Auxiliary Family from Levoglucosenone and Evaluation in the Diels–Alder Reaction. *Synlett* **2018**, *29*, 1441–1446.
78. Klepp, J.; Podversnik, H.; Puschnig, J.; Greatrex, B.W. Diastereoselective sulfa-Michael reactions controlled by a biomass-derived chiral auxiliary. *Tetrahedron Lett.* **2019**, *75*, 3894–3903. [[CrossRef](#)]
79. Sharipov, B.T.; Davydova, A.N.; Faizullina, L.K.; Valeev, F.A. Preparation of the diastereomerically pure 2S-hydroxy derivative of dihydrolevoglucosenone (cyrene). *Mendeleev Commun.* **2019**, *29*, 200–202. [[CrossRef](#)]
80. Martinho, L.A.; Rosalba, T.P.F.; Sousa, G.G.; Gatto, C.C.; Politi, J.R.S.; Andrade, C.K.Z. Cyrene: A very reactive bio-based chiral ketone in diastereoselective Passerini reactions. *Mol. Divers.* **2023**. [[CrossRef](#)] [[PubMed](#)]
81. Hohol, R.E.; Arcure, H.; Witczak, Z.J.; Bielski, R.; Kirschbaum, K.; Andreana, P.; Mencer, D.E. One-pot synthesis of carbohydrate exo-cyclic enones and hemiketals with 6,8-dioxabicyclo- [3.2.1] octane moieties. Serendipitous formation of a spironolactone when 2-pyridinecarboxaldehyde is used as the reactant. Part II\*. *Tetrahedron Lett.* **2018**, *74*, 7303–7309. [[CrossRef](#)]
82. Ray, P.; Hughes, T.; Smith, C.; Hibbert, M.; Saito, K.; Simon, G.P. Development of bio-acrylic polymers from Cyrene™: Transforming a green solvent to a green polymer. *Polym. Chem.* **2019**, *10*, 3334–3341. [[CrossRef](#)]
83. Néant, F.D.; Mouterde, L.; Fadlallah, S.; Miller, S.A.; Allais, F. Sustainable Synthesis and Polycondensation of Levoglucosenone-Cyrene-Based Bicyclic Diol Monomer: Access to Renewable Polyesters. *ChemSusChem* **2020**, *10*, 1002.
84. Fadlallah, S.; Peru, A.A.M.; Allais, L.L.F. Chemo-enzymatic synthesis of a levoglucosenone-derived bi-functional monomer and its ring-opening metathesis polymerization in the green solvent Cyrene™. *Polym. Chem.* **2020**, *11*, 7471. [[CrossRef](#)]
85. Stini, N.A.; Gkizis, P.L.; Kokotos, C.G. Cyrene: A bio-based solvent for the Mizoroki–Heck reaction of aryl iodides. *Org. Biomol. Chem.* **2023**, *21*, 351. [[CrossRef](#)] [[PubMed](#)]

86. Galaverna, R.S.; Fernandes, L.P.; Silva, V.H.M.; Siervo, A.; Pastre, J.C. Humins-Like Solid Support for Palladium Immobilization: Highly Efficient and Recyclable Catalyst for Cross-Coupling reactions. *Org. Chem.* **2022**, *24*, 47–57. [[CrossRef](#)]
87. Ferrazzano, L.; Martelli, G.; Fantoni, T.; Daka, A.; Corbisiero, D.; Viola, A.; Ricci, A.; Cabri, W.; Tolomelli, A. Fast Heck-Cassar-Sonogashira (HCS) Reactions in Green Solvents. *Org. Lett.* **2020**, *22*, 3969–3973. [[CrossRef](#)]
88. Mistry, L.; Mapesa, K.; Bousfield, T.W.; Camp, J.E. Synthesis of Ureas in the Bio-alternative Solvent Cyrene. *Green Chem.* **2017**, *19*, 2123–2128. [[CrossRef](#)]
89. Wilson, K.L.; Murray, J.; Jamieson, C.; Watson, A.J.B. Cyrene as a Bio-Based Solvent for the Suzuki-Miyaura Cross Coupling. *Synlett* **2018**, *29*, 650–654.
90. Sherwood, J. Suzuki–Miyaura cross coupling is not an informative reaction to demonstrate the performance of new solvents. *Org. Chem.* **2020**, *16*, 1001–1005. [[CrossRef](#)]
91. Mention, M.M.; Flourat, A.L.; Peyrot, C.; Allais, F. Biomimetic regioselective and high-yielding Cu(I)-catalyzed dimerization of sinapate esters in green solvent Cyrene<sup>TM</sup>: Towards sustainable antioxidant and anti-UV ingredients. *Green Chem.* **2020**, *22*, 2077–2085. [[CrossRef](#)]
92. Marathianos, A.; Liarou, E.; Hancox, E.; Grace, J.L.; Haddleton, D.M. Dihydrolevoglucosenone (Cyrene<sup>TM</sup>) as a biorenewable solvent for Cu(0)wire-mediated reversible deactivation radical polymerization (RDRP) without external deoxygenation. *Green Chem.* **2020**, *22*, 5833. [[CrossRef](#)]
93. Veerabagu, U.; Jaikumar, G.; Lu, F.S.; Quero, F. High yield and greener C-H difluoromethylation reactions using copper iodide nanoparticles/boron nitride nanosheets as versatile and recyclable heterogeneous catalyst. *React. Chem. Eng.* **2021**, *6*, 1900–1910. [[CrossRef](#)]
94. Nickisch, R.; Conen, P.; Gabrielsen, S.M.; Meier, M.A.R. A more sustainable isothiocyanate synthesis by amine catalyzed sulfurization of isocyanides with elemental sulfur. *RSC Adv.* **2021**, *11*, 3134–3142. [[CrossRef](#)]
95. Sangon, S.; Supanchaiyamat, N.; Sherwood, J.; McElroy, C.R.; Hunt, A.J. Direct comparison of safer or sustainable alternative dipolar aprotic solvents for use in carbon-carbon bond formation. *Chem. Eng.* **2020**, *5*, 1798. [[CrossRef](#)]
96. Wilson, K.L.; Murray, J.; Jamieson, C.; Watson, A.J.B. Cyrene as a bio-based solvent for HATU mediated amide coupling. *Org. Biomol. Chem.* **2018**, *16*, 2851–2854. [[CrossRef](#)]
97. Bousfield, T.W.; Pearce, K.P.R.; Nyaminia, S.B.; Dimakisa, A.A.; Camp, J.E. Synthesis of Amides from Acid Chlorides and Amines in the Bio-based Solvent Cyrene<sup>TM</sup>. *Green Chem.* **2019**, *21*, 3675–3681. [[CrossRef](#)]
98. De Bruyn, M.; Budarin, V.L.; Misefari, A.; Shimizu, S.; Fish, H.; Cockett, M.; Hunt, A.J.; Hofstetter, H.; Weckhuysen, B.M.; Clark, J.H. Geminal Diol of Dihydrolevoglucosenone as a Switchable Hydrotrope: A Continuum of Green Nanostructured Solvents. *ACS Sustain. Chem. Eng.* **2019**, *7*, 7878–7883. [[CrossRef](#)]
99. Abranches, D.O.; Benfica, J.; Shimizu, S.; Coutinho, J.A. The Perspective of Cooperative Hydrotrophy on the Solubility in Aqueous Solutions of Cyrene. *Ind. Eng. Chem. Res.* **2020**, *10*, 0888–5885. [[CrossRef](#)]
100. Chen, Y.; Terazono, Y.C.; Fefer, M.; Liu, J.; Gale, C.B.; Brook, M.A. A simple route to photodynamic chlorin e6 amide derivatives. *J. Porphyr. Phthalocyanines* **2022**, *26*, 56–64. [[CrossRef](#)]
101. Lawrenson, S.; North, M.; Peigneguy, F.; Routledge, A. Greener solvents for solid-phase synthesis. *Green Chem.* **2017**, *19*, 952. [[CrossRef](#)]
102. Ferrazzano, L.; Corbisiero, D.; Martelli, G.; Tolomelli, A.; Viola, A.; Ricci, A.; Cabri, W. Green Solvent Mixtures for Solid-Phase Peptide Synthesis: A Dimethylformamide-Free Highly Efficient Synthesis of Pharmaceutical-Grade Peptides. *ACS Sustain. Chem. Eng.* **2019**, *7*, 11036–11043.
103. Camp, J.E.; Nyaminia, S.B.; Scott, F.J. Cyrene<sup>TM</sup> is a green alternative to DMSO as a solvent for antibacterial drug discovery against ESKAPE pathogens. *RSC Med. Chem.* **2020**, *11*, 111. [[CrossRef](#)] [[PubMed](#)]
104. Mouterde, L.M.M.; Couvreur, J.; Langlait, M.M.J.; Brunois, F.; Allais, F. Identification and expression of a CHMO from the *Pseudomonas aeruginosa* strain Pa1242: Application to the bioconversion of Cyrene<sup>TM</sup> into a key precursor (S)- $\gamma$ -hydroxymethylbutyrolactone. *Green Chem.* **2021**, *23*, 2694. [[CrossRef](#)]
105. Andrew, O.B.; Sherwood, J.; Hurst, G.A. A Greener Synthesis of the Antidepressant Bupropion Hydrochloride. *J. Chem. Educ.* **2022**, *99*, 3277–3282. [[CrossRef](#)]
106. Citarella, A.; Amenta, A.; Passarella, D.; Micale, N. Cyrene: A Green Solvent for the Synthesis of Bioactive Molecules and Functional Biomaterials. *Int. J. Mol. Sci.* **2022**, *23*, 15960. [[CrossRef](#)] [[PubMed](#)]
107. Witczak, Z.J.; Bielski, R.; Mencer, D.E. Concise and efficient synthesis of E-stereoisomers of exo-cyclic carbohydrate enones. Aldol condensation of dihydrolevoglucosenone with five-membered aromatic aldehydes 1 Part 1. *Tetrahedron Lett.* **2017**, *58*, 4069–4072. [[CrossRef](#)]
108. Yu, H.T.; Yu, D.K.; Xue, Z.M.; Zhang, B.L. Dihydrolevoglucosenone as a bio-based catalytic solvent for efficient reductive-transformation of CO<sub>2</sub> with amines into formamides and benzothiazoles. *J. Chem. Eng.* **2022**, *431*, 133397. [[CrossRef](#)]
109. Gonzalo, G. Biocatalysed reductions of  $\alpha$ -ketoesters employing Cyrene<sup>TM</sup> as cosolvent. *Biocatal. Biotransformation* **2022**, *40*, 252–257. [[CrossRef](#)]
110. Guajardo, N.; María, P.D. Assessing biocatalysis using dihydrolevoglucosenone (Cyrene<sup>TM</sup>) as versatile bio-based (co)solvent. *Mol. Catal.* **2020**, *485*, 110813. [[CrossRef](#)]

111. Kuhl, N.; Turnbull, B.W.H.; Thaisrivongs, D.A.; Ji, Y.N.; Larson, R.T.; Shevlin, M.; Prier, C.K.; Chung, C.K.; Desmond, R.; Guetschow, E.; et al. Utilizing biocatalysis and a sulfolane-mediated reductive acetal opening to access nemtabrutinib from Cyrene. *Green Chem.* **2023**, *25*, 606. [[CrossRef](#)]
112. Tamargo, R.J.I.; Rubio, P.Y.M.; Mohandoss, S.; Shim, J.J.; Lee, Y.R. Cyrene™ as a Neoteric Bio-Based Solvent for Catalyst-Free Microwave-Assisted Construction of Diverse Bipyridine Analogues for Heavy-Metal Sensing. *ChemSusChem* **2021**, *14*, 2133–2140. [[CrossRef](#)]
113. Alammari, A.; Park, S.H.; Ibrahim, I.; Arun, D.; Holtzl, T.; Dumée, L.F.; Lim, H.N.; Szekeley, G. Architecting neonicotinoid-scavenging nano-composite hydrogels for environmental remediation. *Appl. Mater. Today* **2020**, *21*, 100878. [[CrossRef](#)]
114. Grune, C.; Thamm, J.; Werz, O.; Fischer, D. Cyrene™ as an Alternative Sustainable Solvent for the Preparation of Poly(lactic-co-glycolic acid) Nanoparticles. *J. Pharm. Sci.* **2021**, *110*, 959–964. [[CrossRef](#)] [[PubMed](#)]
115. Czapka, A.; Grune, C.; Schädel, D.P.; Bachmann, V.; Scheuer, K.; Dirauf, M.; Weber, C.; Skaltsounis, A.L.; Jandt, K.D.; Schubert, U.S.; et al. Drug delivery of 6-bromoindirubin-3'-glycerol-oxime ether employing poly(D,L-lactide-co-glycolide)-based nanoencapsulation techniques with sustainable solvents. *J. Nanobiotechnol.* **2022**, *20*, 5. [[CrossRef](#)] [[PubMed](#)]
116. German, L.; Cuevas, J.M.; Cobos, R.; Alvare, L.P.; Vilela, J.L.V. Green alternative cosolvents to N-methyl-2-pyrrolidone in water polyurethane dispersions. *RSC Adv.* **2021**, *11*, 19070. [[CrossRef](#)]
117. Adama, J.; Sorbob, M.R.D.; Kaur, J.; Romano, R.; Singh, M.; Altucci, C. Surface Interactions Studies of Novel Two-Dimensional Molybdenum Disulfide with Gram-Negative and GramPositive Bacteria. *Anal. Lett.* **2023**, *56*, 357–371. [[CrossRef](#)]
118. Itawi, H.E.; Fadlallah, S.; Perré, P.; Leephakphumphanich, W.; Ruscassier, N.; Zoghalmi, A.; Allais, F.; Perré, P. Online Microfluidic Production of Sustainable Cyrene™-Derived Porous Microparticles. *Sustainability* **2023**, *15*, 2023. [[CrossRef](#)]
119. Bai, Y.C.; Hawley, W.B.; Jafta, C.J.; Muralidharan, N.; Polzin, B.J.; Belharouak, I. Sustainable recycling of cathode scraps via Cyrene-based separation. *Sustain. Mater. Technol.* **2020**, *25*, e00202. [[CrossRef](#)]
120. Zhou, H.; Pei, B.; Fan, Q.L.; Xin, F.X. Whittingham, Can Greener Cyrene Replace NMP for Electrode Preparation of NMC 811 Cathodes? *J. Electrochem. Soc.* **2021**, *168*, 040536. [[CrossRef](#)]

**Disclaimer/Publisher's Note:** The statements, opinions and data contained in all publications are solely those of the individual author(s) and contributor(s) and not of MDPI and/or the editor(s). MDPI and/or the editor(s) disclaim responsibility for any injury to people or property resulting from any ideas, methods, instructions or products referred to in the content.